(2)

DOT/FAA/SA-89/4

Advanced System
Acquisition Service
Washington, D.C. 20591

Turbulence Spectral Widths View Angle Independence as Observed by Doppler Radar

J. T. Lee and
K. Thomas

Cooperative Institute for Mesoscale Meteorological Studies
University of Oklahoma
401 East Boyd
Norman, OK 73019

October 1989

Final Report

U.S. Department of Transportation
Federal Aviation Administration

DISCLAIMER NOTICE

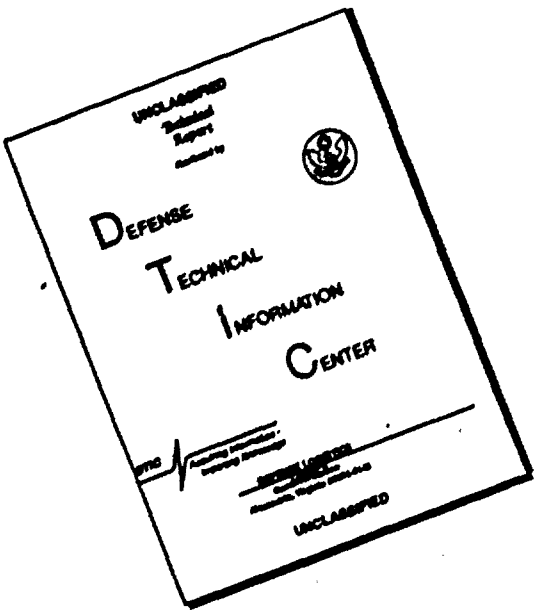

THIS DOCUMENT IS BEST QUALITY AVAILABLE. THE COPY FURNISHED TO DTIC CONTAINED A SIGNIFICANT NUMBER OF PAGES WHICH DO NOT REPRODUCE LEGIBLY.

Technical Report Documentation Page

1. Report No.	2. Government Accession No.	3. Recipient's Catalog No.
DOT/FAA/ SA-~~89/2~~ 89/4		

4. Title and Subtitle	5. Report Date
Turbulence Spectral Widths View Angle Independence as Observed by Doppler Radar	October 1989
	6. Performing Organization Code: CIMMS
7. Author(s): J. T. Lee and K. Thomas	8. Performing Organization Report No.
9. Performing Organization Name and Address: Cooperative Institute for Mesoscale Meteorological Studies / University of Oklahoma, 401 East Boyd, Norman, OK 73019	10. Work Unit No. (TRAIS)
	11. Contract or Grant No.: DTFA01-8C-Y-10524
12. Sponsoring Agency Name and Address: U.S. Department of Transportation, Federal Aviation Administration, Advanced System Acquisition Service, Washington, DC 20591	13. Type of Report and Period Covered
	14. Sponsoring Agency Code: ASA-220

15. Supplementary Notes

16. Abstract

As air traffic density increases, effective use of airspace must include consideration of weather. Accurate identification of turbulent volumes is of paramount importance to flight safety. The advent of Doppler radar has made it possible to observe wind motion in convective clouds. Over a number of years, research has lead to the spectral width (standard deviation) of the Doppler velocity measurements as an indicator of turbulence. In this paper we address the hypotheses that turbulence is essentially isotropic in convective systems, and therefore, observations of turbulence are independent of viewing angle.

Radar observations made during the months of April, May, and June in 1980-1985 were scanned to locate storms amenable to analysis. A number of cases are presented in which a dual-Doppler network provided the essential data. Each case is in a different quadrant with respect to the Norman Doppler. Forty-four horizontal planes were studied from six different storms. The results of four of these storms are presented. Maximum reflectivity of these storms range from 51 to 58 dBZ. Altitudes included in this study range from near surface to 7 km. At these altitudes the maximum spectral width was 12 ms^{-1} . For these cases, involving nearly 30,000 data points, 70% of the spectral width observations from CIM and NRO were within 1 ms^{-1} or less. These results indicate that the use of Doppler radar to detect turbulent regions within thunderstorms has a high probility of success, and the turbulent regions can be detected independent of the direction from which they are viewed.

17. Key Words	18. Distribution Statement
Doppler radar, turbulence, spectral width	This document is available to the public through the National Technical Information Service, Springfield, Virginia 22161.

19. Security Classif. (of this report)	20. Security Classif. (of this page)	21. No. of Pages	22. Price
UNCLASSIFIED	UNCLASSIFIED	47	

Form DOT F 1700.7 (8-72) Reproduction of completed page authorized

PREFACE

The authors wish to express their appreciation to Drs. D. S. Zrnic' and R. J. Doviak for their review, suggestions, and support. We are indebted to Ms. Joan Kimpel for the excellent art work, and to Ms. Sana Bahouth for the typing. This work was supported under FAA contract DTFAO1-80-Y-10524.

TABLE OF CONTENTS

ABSTRACT

As air traffic density increases, effective use of airspace must include consideration of weather. Accurate identification of turbulent volumes is of paramount importance to flight safety. The advent of Doppler radar has made it possible to observe wind motion in convective clouds. Over a number of years, research has lead to the spectral width (standard deviation) of the Doppler velocity measurements as an indicator of turbulence. In this paper we address the hypothesis that turbulence is essentially isotropic in convective systems, and therefore, observations of turbulence are independent of viewing angle.

Radar observations made during the months of April, May, and June in 1980-1985 were scanned to locate storms amenable to analysis. A number of cases are presented in which a dual-Doppler network provided the essential data. Each case is in a different quadrant with respect to the Norman Doppler. Forty-four horizontal planes were studied from six different storms. The results of four of these storms are presented. Maximum reflectivity of these storms range from 51 to 58 dBZ. Altitudes included in this study range from near surface to 7 km. At these altitudes the maximum spectral width was 12 ms^{-1}. For these cases, involving nearly 30,000 data points, 70% of the spectral width observations from CIM and NRO were within 1 ms^{-1}, and 88% had a difference of 2 ms^{-1} or less. These results indicate that the use of Doppler radar to detect turbulent regions has a high probability of success, and the turbulent regions can be detected independent of the direction from which they are viewed.

List of Figures

LIST OF TABLES

TURBULENCE SPECTRAL WIDTHS VIEW ANGLE INDEPENDENCE AS OBSERVED BY DOPPLER RADAR

J. T. Lee and K. Thomas
Cooperative Institute for Mesoscale Meteorological Studies
University of Oklahoma
401 East Boyd
Norman, OK 73019

1. INTRODUCTION

Aircrafts usually avoid large areas of airspace occupied by thunderstorms resulting in service disruption and increased fuel consumption. At times this means missed connections and/or cancelled flights. The economic considerations may influence decisions as to flight paths which may turn out to be a disadvantage to aircraft, crew, and passengers. The advent of Doppler radar offers an important new capability for addressing this problem.

Over a number of years, cooperative programs between the Federal Aviation Administration (FAA), the United Stated Air Force (USAF) through the Air Force Cambridge Research Laboratory (AFCRL) and the Aeronautical Systems Division (ASD), the National Aeronautics and Space Administration (NASA), universities, including Massachusetts Institute of Technology's Lincoln Laboratory, the National Center for Atmopsheric Research (NCAR) and the National Oceanic and Atmospheric Administration's National Severe Storms Laboratory (NSSL) have been conducted to observe thunderstorm turbulence with aircraft and Doppler radar.

The results of these programs have been published (Lee, 1967; Burnham

and Lee, 1969; Lee and Carpenter, 1979; Doviak and Lee, 1985). It was shown that turbulence experienced by aircraft could be related to the spectral width of the radial velocity measured by the Doppler radar (Donaldson and Wexler, 1969; Lee, 1977; Labitt, 1981; Bohne, 1982; Lee, Y., et al, 1985; and others). It was also found that spectral widths corresponding to turbulence greater than moderate were observed in only about 30% of the volume of a tornadic storm -- that is 70% of the storm may have only light-to-moderate turbulence (Doviak et al., 1978). If the intensity and location of turbulence can be accurately and routinely detected by ground based Doppler radar, aircraft can be safely routed around the hazardous regions (Zrnic' and Lee, 1982; Mahapatra and Lee, 1984).

The viewing angle independence is thus important. Spectral width is a scaler parameter which, in isotropic turbulence, is independent of the radar's viewing angle. One purpose of this study is to examine to what extent the turbulence in the storms is nearly isotropic. This is accomplished by comparing spectral width measurements made by two Doppler radars separated by tens of kilometers, and viewing the same storm from a different angle.

2. SPECTRAL WIDTH

Atmospheric turbulence in convective clouds is a fluctuation of the wind around a mean value. These fluctuations are caused by mechanical and/or thermal forces acting independently or in concert. In a turbulent flow, turbulent energy is assumed to cascade from the longer wavelengths (large eddy sizes) to the shorter wavelengths (smaller eddy sizes) in a dissipation process (MacCready, 1964; Frisch and Strauch, 1976; Gage, 1979; Lilly and Peterson, 1983; Brewster and Zrnic', 1986).

Doppler radar can measure these variations in the observable wind field. These variations within a resolution volume will result in an increase in the spectral width of the Doppler-estimated mean wind.

The Doppler radar's spectral width estimation is a function of radar system parameters (Zrnic', 1977 and 1979) and meteorological factors. There are four major mechanisms which can effectively broaden the spectral widths -- that is, increase its numerical value. These are: antenna angular velocity rotation (r), differences in drop sizes (d), and therefore, differences in fall speeds, radial velocity shears (s), and turbulence (t). This relationship is expressed as:

$$s^2(\text{total}) = s^2(r) + s^2(d) + s^2(s) + s^2(t),$$

where $s^2(\text{total})$ is the total spectral width squared. The beam broadening terms, as well as the effect of drop size distributions, have been evaluated by a number of researchers (Nathanson, 1969; Lhermitte, 1963; Doviak et al., 1979). These studies indicate that the contributions by beam broadening (antenna rotation) and different drop size distributions can effectively be neglected. However, there exist certain conditions of strong shear that will cause the shear term to be significant.

In this study, we will assume that the turbulence is homogeneous within the resolution volume, defined as that volume within the half-power interval of the radiated beam and the depth of the individual sampling interval. For further discussion of turbulence and resolution volume see Doviak and Zrnic' (1984) and Istok and Doviak (1986).

To utilize this information and to test if the turbulence is isotropic or nearly isotropic, and therefore independent of viewing angle, a series of observations were made using a configuration of two Doppler radars. This

dual-Doppler network is shown in Figure 1. The radars located at NSSL in Norman (NRO) and at Page Field (formerly Cimarron Airport) (CIM) are separated by 41.473 km. CIM is on the 310.08 deg. radial (true) from NRO. The individual characteristics of these radars are given in Table 1.

The Dopper data are processed as detailed in Appendix A. Generally the data are assigned to grid points spaced at 1 km intervals (Brown et al, 1981), both in the vertical and the horizontal. A Cressman spherical objective analysis scheme is used with a 1 or 1.5 km radius of influence, depending on the Doppler radar scanning strategy on a particular day. A minimum of two data points from the same radar is required for inclusion. Areas of insufficient data are deleted. Data in regions where the reflectivity is less than 20 dBZ are not used in the final analysis because of possible noise contamination.

The following cases are presented to illustrate the independence of spectral width from viewing angle restrictions.

3. TEST CASES

A number of cases were studied. Four are presented which illustrate various viewing angles, different ranges, and several elevation angles. Each case is in a different quadrant from the Norman radar. Figure 2 shows the relative position of these storms and the Doppler radars.

3.1 May 17, 1983

On May 17, 1983, the synoptic situation supports a strong southwesterly flow aloft and a dryline in western Oklahoma. Thunderstorms (some tornadic) first develop in southwestern Kansas. Others soon develop in northwest Oklahoma. These thunderstorms move eastward and new cells develop southward, forming a NNE-SSW line. By

Table 1 NSSL Doppler Radar Characteristics

PARAMETER	CIMARRON (CIM)	NORMAN (NRO)
Antenna		
Shape	Parabolic	Parabolic
Diameter	9.15 m	9.15 m
Half-Power Beamwidth	0.85 deg.	0.81 deg.
Gain	46 dB	46.8 dB
First Side-Lobe Level	21 dB	21 dB
Polarization	Vertical	Vertical
RMS Surface Deviation	2.5 mm	2.8 mm
Transmitter		
Wavelength	10.94 cm	10.52 cm
Frequency	2735 MHz	2850 MHz
Peak Power	500 kW	750 kW
Pulse Width	1 μs (150 m)**	1 μs (150 m)**
Pulse Repetition Time (PRT)	See below	See below
Receiver		
System Noise Figure	4 dB	4 dB
Transfer Function	Doppler - linear Intensity - logarithmic	Doppler - linear Intensity - logarithmic
Dynamic Range	80 dB	80 dB
Bandwidth: 3 dB; 6 dB	0.6; 0.85 MHz	0.6; 0.85 MHz
Receiver Noise Level	-105 dBM	-108 dBM

Basic PRT	Unambiguous CIM/NRO Velocity	Velocity Range	Velocity Range Increment	Intensity Max Range*	Intensity Range Increment*	Digital Tape Density
768 μs	35.6/34.2 ms^{-1}	115 km	150 m	460 km	600 m	744 bpi
922 μs	29.7/28.5 ms^{-1}	138 km	180 m	552 km	720 m	620 bpi
1075 μs	25.4/24.5 ms^{-1}	161 km	210 m	644 km	840 m	531 bpi
1229 μs	22.3/21.4 ms^{-1}	184 km	240 m	736 km	960 m	465 bpi

* Values given are for batch; in equi-spaced mode the intensity range coverage is same as velocity.

** In wide-pulse mode, pulse width is 3 μs or 5 μs; PRT is three times one of the above four basic PRT's (usually 768 μs). Equi-spaced pulses only.

1628 CST, this line moves to about 40 km northwest of Norman.

Figure 3 is a photograph of the 10-cm WSR-57 weather radar PPI display. This radar is located at Norman adjacent to the Doppler radar. The storm covered by the dual-Doppler observations is located at A, at 265°/50 km from NRO, and 208°/38 km from CIM. Thus the beams intersect at an angle of 41°. Beam width at this range is 0.7 km for NRO and 0.5 km for CIM. Maximum reflectivity factor of the storm at this time is 54 dBZ. The maximum total spectral width (σ) is 10 ms^{-1}.

The dual-Doppler data are processed and grided. Six horizontal planes - surface (lowest elevation available) 1, 2, 3, 4, and 5 km above ground, with approximatelv 10,000 data points - are examined. Initially the NRO and CIM reflectivities are compared and cross-correlated to establish if there are any range or azimuth discrepancies besides the ones accounted for by calibrations. For May 17th, a maximum correlation coefficient of 97% is observed for a 0,0 lag. In Figure 4 we show the radar reflectivity at 2 km, as seen by the Cimarron radar. Figure 5 is the corresponding correlation coefficient as the data are lagged in both the x and y directions. Results are similar at other altitudes, therefore no range or azimuth correction is applied to these data. The distribution of the differences between the corresponding reflectivity values for all data points is given in Figure 6, and we shall thus assume that the radars are observing the same volumes.

The corresponding analysis is then performed on the spectral widths. Figure 7 is an example of the spectral width field for the 2 km level, as observed by the CIM radar. In the portion of the storm displayed in Figure 7, the spectral width varies from 2 to 9 ms^{-1}, with 4 ms^{-1} being the dominant value. Note that in the region of 50 dBZ reflectivity values in

Figure 4 (coordinates x = -19.14 and y = -27.7), the corresponding spectral widths are 3-4 ms^{-1}, indicating light-to-moderate turbulence (Donaldson and Wexler, 1969; Lee, 1979). Some of the large spectral widths of 9 ms^{-1} at x = -24.14 and y = 45.7 are most probably due to artifacts at low signal strength. Figure 8 shows the corresponding differences between the CIM and NRO observations. In general, these differences are within ± 2 ms^{-1}. A few 4 ms^{-1} values at x = -57 , y = +7 and at x = -57, y = -16 are at the edges of the storm and are the result of contamination of the NRO radar data by noisy signal. Similar comparisons are made for the other five horizontal planes. These results are combined and summarized in Figure 9. The heavy black line is for all the data. Note that more than 70% of the observations are within 1 ms^{-1}, and 86% are within 2 ms^{-1}. In this figure we also show the distribution of the differences classified according to reflectivity. From this figure, there appears to be very little reflectivity dependence. Thus is this storm, with reflectivities ranging up to 54 dBZ and at altitudes up to 5 km, the observed spectral widths obtained by NRO and CIM are essentially the same when compared point-by-point.

The vertical motion in the storm is calculated from the dual-Doppler data following the method of Brown, et al. (1981). Figure 10 shows the relative position of the radar reflectivity contours, areas of significant spectral widths, and the vertical motion fields. Particular notice should be made that the areas of maximum reflectivities are not necessarily colocated with the areas of maximum spectral widths. Indications are that the turbulence is more closely associated with the edge of updrafts and downdrafts. Frisch and Strauch (1976), and Knupp and Cotton (1982) showed similar patterns. The future of forecasting turbulent areas may

well depend on the success in detailing these vertical motions within the storm.

3.2 May 25, 1983

On 25 May 1983, moist, unstable air is brought into central Oklahoma by low-level southeasterly winds. Surface dew points are near 14 °C. A north westerly wind at 500 mb guides a cold front from northern Oklahoma through Norman and Tulsa by mid-afternoon. Thunderstorms form on the front east of Norman and the main center of activity is 120 km southeast of Norman at 1700 CST. The storm covered by the dual-Doppler observations is at 138°/103 km from NRO, and 135°/144 km from CIM. The radar beams intersect at an angle of 3°. The NRO beamwidth at the storm is 1.4 km and corresponding value for CIM is 1.9 km. In this case, CIM is looking almost directly over the shoulder of NRO. Figure 11 is a photograph of the WSR-57 radar scope at 0° elevation angle at 1707 CST. Maximum reflectivity of the storm is 58 dBZ and the spectral widths vary from 2 to 10 ms^{-1}. Due to the greater distance from CIM on May 17th, the lowest usable plane is at 3 km. Data for 3, 4, 5, 6, and 7 km are used in the analysis. Approximately 12,000 data points are in the grid.

Again we test the radars for range and azimuth consistency and obtain a maximum correlation coefficient of 97% at 0,0 lag (Figure 12).

Figure 13 is a portion of the spectral width field at 5 km, as observed by CIM. For this case the widths are generally larger (7, 8, and 9 ms^{-1}) than in the previous case. This is to be expected since the storm as a whole is more intense than the one on May 17th. Figure 14 shows the cross correlation coefficients for the spectral widths for CIM and NRO at 5 km. The 69% value at 0,0 lag is not as large as for the reflectivity, but

is still acceptable. Figure 15 is the corresponding difference field (NRO-CIM). Here again we find good correspondence, with 82% of the differences within $\pm$ 1 ms^{-1} and 96% within 2 ms^{-1} or less.

This is even better than May 17th even though the CIM beamwidth is about 0.5 km more than NRO's due to the greater distance to the storm from CIM. The high correspondence is very encouraging.

3.3 May 27, 1983

For 27 May 1983, northwesterly flow at 500 mb continues to dominate the state. At the surface the air is moist (dew point about 15°C) and unstable. There is a north-south quasi-stationary front in eastern Oklahoma with strong southerly winds to the west of the front, including the Oklahoma City area. In late afternoon several thunderstorms form northeast of Oklahoma City. Dual-Doppler coverage at 1740 CST is centered on a storm at 40° and 64 km from Norman. From CIM the azimuth and range is 70° and 76 km. The NRO beamwidth near the storm is 0.85 km and CIM's is 1.02 km. These beams intersect at an angle of 32°. Maximum reflectivity of the storm is 51 dBZ and 3/4 inch hail is reported to be associated with this storm. Maximum spectral width observed is 8 ms^{-1}.

Figure 17 shows the WSR-57 radar display (0° tilt angle) for 1743 CST. Data from four altitudes -- near the surface (lowest elevation angle), 1, 2, and 3 km -- are available. The lowest altitude is not used because of contamination of the CIM data by returns from ground objects (ground clutter). A total of over 700 data points are used. This storm is unique in that it is an isolated storm and the possibility of second trip and sidelobe contamination is minimized. This means that the analysis is straightforward and very little editing is required.

Figure 18 illustrates the correlation between the NRO and CIM

reflectivity fields at an altitude of 2 km. Once again the highest correlation is at 0,0 lag, indicating that there has been no detectable shift in range or azimuth of the radar data. The corresponding 2 km CIM reflectivity field is shown in Figure 19. This storm is basically one major cell located at x = 68, y = 28. Figure 20 is the spectral width field with 3 to 4 ms^{-1} being the predominant values, except near the northwest edge of the storm where a few 6 ms^{-1} are found. As seen in Figure 21, which shows the difference in the spectral widths values between the CIM and NRO observations, this northwest area also has the largest difference. Most other areas have values near 0 ms^{-1}. The graph (Figure 22) shows this good agreement between the CIM and NRO widths, with nearly 80% of the observational differences 1 ms^{-1} or less and 98% 2 ms^{-1} or less.

3.4 May 28, 1983

On 28 May 1983, the 500 mb flow is from the northwest. Moist, unstable air is moving northward over the state during the day, while the remnants of a mesoscale convective complex (MCC; large area of thunderstorms) is moving into western Oklahoma from eastern New Mexico and eastern Colorado. These storms, on an east northeast/west southwest line, increased in intensity and by 1408 CST the leading edge was about 120 km northwest of Norman. The storm selected for analysis is 317° at 118 km from NRO, and 320° at 78 km from CIM. The beams intersect making an angle of 3°. In this case, NRO is looking over the shoulder of CIM -- the reverse of the May 25th case. The NRO radar beamwidth at the storm is 1.6 km and CIM's is 1.0 km. Maximum reflectivity of the storm is 55 dBZ. Maximum spectral width is 12 ms^{-1}. Figure 23 is the 2008 CST for 28 May WSR-57 radar scope at 0° elevation angle. Seven altitude

sections (1, 2, 3, 4, 5, 6, and 7 km) are analyzed.

In Fig. 24 are the cross correlation coefficients for the reflectivities and in Figs. 25 and 26 are the CIM spectral widths and the NRO-CIM spectral width differences at 3 km. Once again we note in Figure 24 that the maximum correlation coefficient is near the 0,0 lag, but a slight drift in the radar range/azimuth stability begins to show itself. This particular system is contaminated by large areas of second trip data, but the storm is of such dimension that over 9,000 data points are available for comparison. The section of the storm's spectral width observations, shown in Figure 25, has values of 1 to 9 ms^{-1} -- probably the largest range of values for any of the cases. We note that the spectral width differences in Figure 26 indicate no particular bias for either radar, but the differences are greater than in the previous cases, with only 58% within 1 ms^{-1} or less and 78% within 2 ms^{-1} (Figure 27).

This larger difference can be ascribed to the greater range to the storm (and thus the greater beamwidth) and to the fact that there is so much range-overlaid (second trip data) which was not flagged by the computer program (Brown, et al., 1981). This increase in spectral width differences at long range here and on May 25th suggests that a possible range limitation may have to be determined.

4. SUMMARY

Whereas only a small portion of the analyzed data fields have been presented, the summary graphs (Figures 9, 16, 22 and 27) show that there is strong evidence that turbulence (spectral widths), as detected by ground-based calibrated radar, is independent of viewing angle.

Figure 28 is a composite of all the data for these cases. It

encompasses altitudes from near ground level to 7 km and ranges to storms from 35 km to 120 km. These nearly 30,000 comparisons show that 70% of the NRO and CIM spectral width observations have a difference of 1 ms^{-1} or less and 88% have a difference of 2 ms^{-1} or less. The mean of the distribution is -0.05 ms^{-1}, and the standard deviation is 2.66 ms^{-1}.

At ranges of these storms with reflectivities more than 20 dBZ, the signal-to-receiver noise ratios are larger than 20 dB. This, together with a number of samples processed to obtain σ_v's, implies that errors in individual spectral width estimates from either radar are less than 0.9ms^{-1}. Because at least two estimates from each radar are averaged in the process of interpolating to a 1 x 1 km grid, the statistical errors should be reduced to less than 0.5 ms^{-1}. Thus the small 1 to 2 ms^{-1} differences are real and are most likely due to the short observation period (0.1 s) and slight inconsistencies in the timing of the two observations. There simply may not be sufficient time for a single recording of an isotropic turbulent eddy to perfectly resolve this property. Thus based on the data, we conclude that there prevails -- at least in two dimensions and in moderate-to-severe storms -- isotropy of turbulent eddies with scales less than 1 km. This is important because it means that irrespective of the location of the turbulence, if there are scatters the Doppler radars should be able to delineate the areas. This also suggests that enhanced ability to detect gust fronts and downbursts outflows, which may be turbulent, should be possible by the inclusion of the spectral width in the algorithms, since outflows in themselves may be tangent to the Doppler beam and only detected by the spectral width.

The next step after detection is the problem of forecasting turbulent

areas which may well depend on the success in detailing and modeling the vertical motion within the storm.

APPENDIX

DATA ANALYSIS

The data used for this project were initially processed on the National Bureau of Standards' CYBER 855. Upon completion of the objective analyses, the data were sent to the National Severe Storms Laboratory's VAX 11/780, where the remainder of the analyses were completed. Doppler data were processed using the techniques described by Brown et al. (1981).

Prior to the objective analysis, data for both the Norman Doppler (NRO) and the Cimarron Doppler (CIM) were edited using a local environmental check algorithm (Eilts and Doviak, 1986) and by visual inspection. In the local environmental check, data points are compared to the surrounding data with questionable data points automatically removed.

The data were analyzed using the Cressman (1959) weighting scheme. The radius of influence used was dependent of the data resolution. The grid spacing is 1 km, in the horizontal and vertical. Even with a fairly large vertical influence radius there were a few problems. At extreme distances (140 to 180 km) from the radar site, data points in the vertical may be separated by distances greater than the objective analysis grid spacing of 1 km. This problem occurred with the May 25, 1983 data set, especially with CIM. the May 27th NRO data also fit into this category. At these large distances, the interpolated values may not be representative. Consequently, it was necessary to delete some data values at large distances.

Before any comparisons are performed, several consistency checks are made. Cross correlations between both reflectivity and spectral width

using the analyzed data fields from the two radars are computed. The reason for testing the correlation is to make sure that general features are not displaced in range or azimuth. In this procedure, the data grid of one of the radars is shifted around by 1 km at a time, in both the x and y directions, and new correlations calculated using the following equation:

$$\text{Correlation } [0+d_x,\ 0+d_y]\ (\rho) = \frac{N(\Sigma x Y) - (\Sigma x \Sigma Y)}{[N(\Sigma X^2) - (\Sigma X)^2]^{1/2}\ [N(\Sigma g^2) - (\Sigma y)^2]^{1/2}}$$

where d_x and d_y are displacements in the x and y directions of the CIM data matrix relative to the NRO matrix. Ideally, the best correlations should occur without any shifting of the data (0,0 lag). For this study, data from the two radars correlated quite well except for the May 28, 1983 case where a slight correction had to be included.

The next step involves checking the data for consistency (Brown et al., 1981). In most of the 1983 cases, the NRO and CIM reflectivity values are in agreement.

Histograms are plotted to determine if a correction is needed. In all cases, the NRO and CIM indicates similar distribution of the data, except that the data, at times, contained an error value offset. this error value is calculated and the value added to the NRO data. Although the correction is added to the NRO values, this does not imply that the NRO data are necessarily in error. The corrections used are indicated in the Table 2.

After these corrections are done, a manual check is performed that detects the obvious bad data points. Difference fields of spectral width are then generated and large differences are noted. At these suspect points, both NRO and CIM data are examined and any bad points are deleted.

After this procedure, the data are considered ready for final evaluation and the analysis completed.

Table 1. Corrections applied to NRO Doppler data

Date	Reflectivity Correction	Spectral Width Correction
May 17	+2.4	+0.5
May 25	+7.6	+1.7
May 27	+7.5	+0.0
May 28	+9.7	+1.4

REFERENCES

Bohne, A. R., 1982: "Radar Detection of Turbulence in Precipitation Environments", J. Atmos. Sci., **39**, 1819-1837.

Bohne, A. R., 1981: "Estimation of Turbulence Severity in Precipitation Environments by Radar", 20th Radar Conference, Boston, MA, 446-453.

Brewster, K. A., and D. S. Zrnic', 1986: "Comparison of Eddy Dissipation Rates from Spatial Spectra of Doppler Velocities and Doppler Spectrum Widths", J. Atmos. Oceanic Technol., **3**, 440-452.

Brown, R. A., C. R. Safford, S. P. Nelson, D. W. Burgess, W. C. Bumgarner, M. L. Weible and L. C. Forner, 1981: "Multiple Doppler Radar Analysis of Severe Thunderstorms: Designing a General Analysis System", NOAA Tech. Memo. ERL NSSL-92, National Severe Storms Laboratory, Norman, OK, 18 pp.

Burnham, J., and J. T. Lee, 1969: "Thunderstorm Turbulence and its Relationship to Weather Radar Echoes", J. Aircraft, **6**, 438-445.

Cressman, G. P., 1959: "An Operational Objective Analysis System", Monthly Wea. Review, **87**, 367-374.

Donaldson, R. J., and R. Wexler, 1969: "Flight Hazards in Thunderstorms Determined by Doppler Velocity Variance", J. Appl. Meteor., **8**, 128-133.

Doviak, R. J., D. Sirmans, D. Zrnic', and G. B. Walker, 1975: "Consideration for Pulse-Doppler Radar Observations of Severe Thunderstorms", J. Appl. Meteor., **17**, 189-205.

Doviak, R. J., and J. T. Lee, 1985: "Radar for Storm Forecasting and Weather Hazard Warning", J. Aircraft, **22**, 1059-1063.

Doviak, R. J. and D. S. Zrnic', 1984: Doppler Radar and Weather Observations, Academic Press, New York, N. Y. , 458 pp.

Eilts, M. D., and R. J. Doviak, 1986: "Oklahoma Downbursts and Their Asymmetry", FAA Report No. DOT/FAA/PM-86.

Frisch, A. S. and R. G. Strauch, 1976: "Doppler Radar Measurements of Turbulence Kinetic Energy Dissipation Rates in Northeastern Colorado Convective Storm", J. Appl. Meteor., **15**, 1012-1017.

Gage, K. S., 1979: "Evidence for a K Law Inertial Range in Mesoscale Two-Dimensional Turbulence", J. Atmos. Sci., **36**, 1950-1954.

Istok, M. J. and R. J. Doviak, 1986: "Analysis of the Relation Between Doppler Spectral Width and Thunderstorm Turbulence", J. Atmos. Sci, **43**, 2200-2214

Knupp, K. R., and W. R. Cotton, 1982: "An Intense Quasi-Steady Thunderstorm Over Mountainous Terrain, Part III: Doppler Radar Observations of Turbulent Structure", J. Atmos. Sci., **39**, 359-368.

Labitt, M., 1981: "Coordinated Radar and Aircraft Observations of Turbulence", Project Report ATC-108, Lincoln Laboratory MIT (also FAA Report RD-81-44), 44pp.

Lee, J. T., 1969: "Associations Between Atmospheric Turbulence and Radar Echoes in Oklahoma", NOAA TM ERL NSSL-32, 1, 32 pp.

Lee, J. T., 1977: "Applications of Doppler Radar Turbulence Measurements which Affect Aircraft", FAA Report RD-77-145, 45 pp.

Lee, J. T. and D. M. Carpenter, 1979: "1973-1977 Rough Rider Turbulence - Radar Intensity Study", FAA Report No. FAA-RD-78-115, 17 pp.

Lee, Y., A Paradis, and Diana Klingle-Wilson, 1985: "Preliminary Results of the 1983 Coordinated Aircraft - Doppler Weather Radar Turbulence Experiment", Vol. 1, FAA Report DOT/FAA/PM-86/11, 64 pp.

Lhermitte, R. M., 1963: "Motions of Scatterers and the Variance of the Mean Intensity of Weather Radar Signals", Sperry-Rand Research

Center, 5 RRC-RR-63-57, Sudbury, MA.

Lilly, D. K., and E. L. Peterson, 1983: "Aircraft Measurements of Atmospheric Kinetic Energy Spectra", TELLUS, **35**, 379-382.

MacCready, P. B., Jr., 1964: "Standardization of Gustiness Values from Aircraft", J. Appl. Meteor., **3**, 439-449.

Mahapatra, P. R., and J. T. Lee, 1984: "The Role of NEXRAD in Aircraft Navigation and Flight Safety Enhancement", J. Inst. Navig., **31(1)**, 21-37.

Nathanson, F. E., 1969: Radar Design Principles, McGraw-Hill, New York, N.Y.

Zrnic', D. S., 1977: "Spectral Moment Estimates from Correlated Pulse Pairs", IEEE Trans. Aerosp. Elec. Syst., **AES-13**, 344-354.

Zrnic', D. S., 1979: "Spectrum Width Estimates for Weather Echoes", IEEE Trans. Aerosp. Elec. Syst., **15**, 613-619.

Zrnic', D. S. and J. T. Lee, 1982: "Pulsed Doppler Radar Detects Weather Hazards to Aviation", J. Aircraft, **19**, 183-190.

Zrnic', D. S., R. J. Doviak, J. T. Lee and M. E. Eilts, 1987: "Oklahoma Weather Phenomena That May Effect Aviation" J. Aircraft, **24** (5), 310-316.

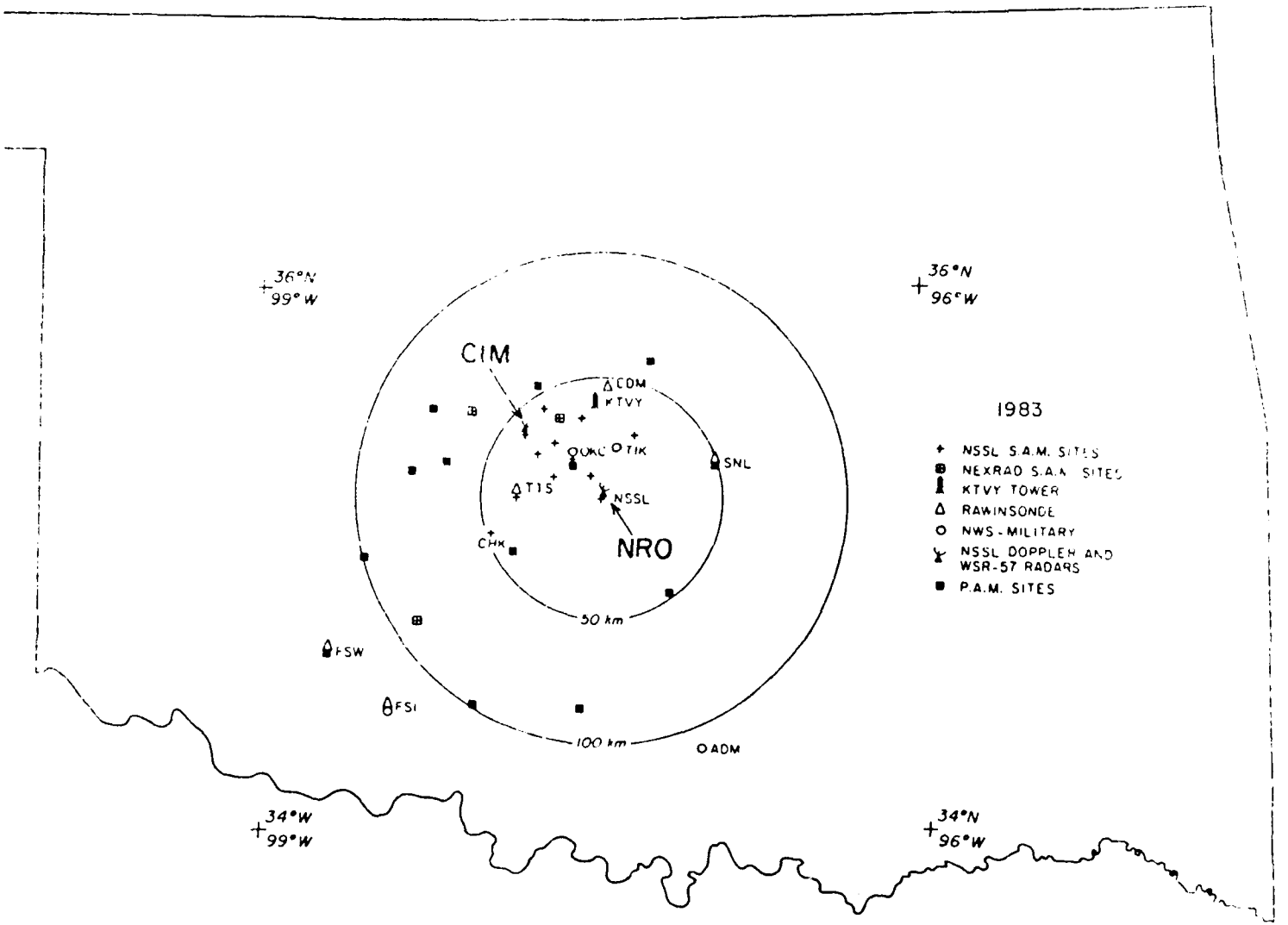

Figure 1 1983 NSSL Spring Program Observational facilities showing dual-Doppler network

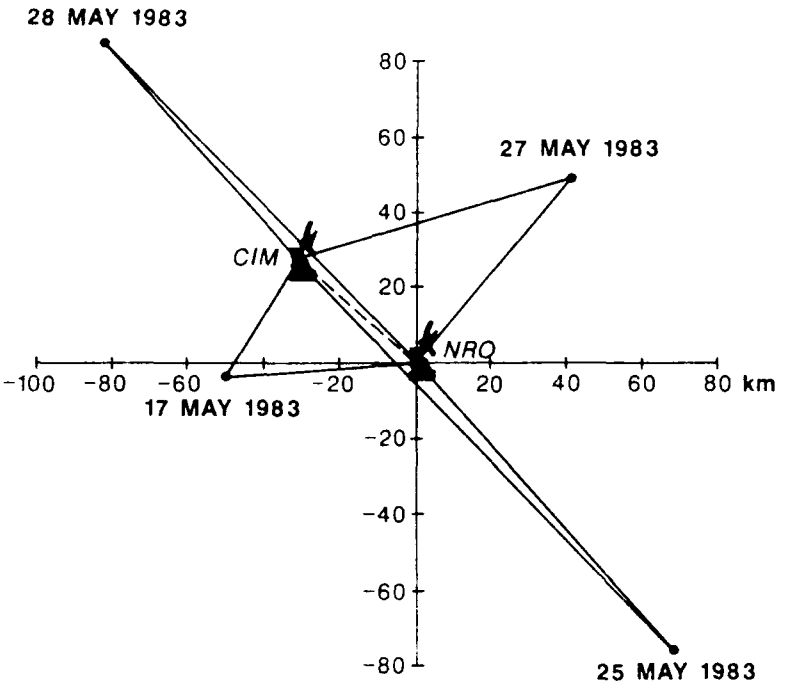

Figure 2 Location and dates of analyzed storms relative to the radar sites at Norman OK (NRO) and Page Field, Oklahoma City, OK (CIM)

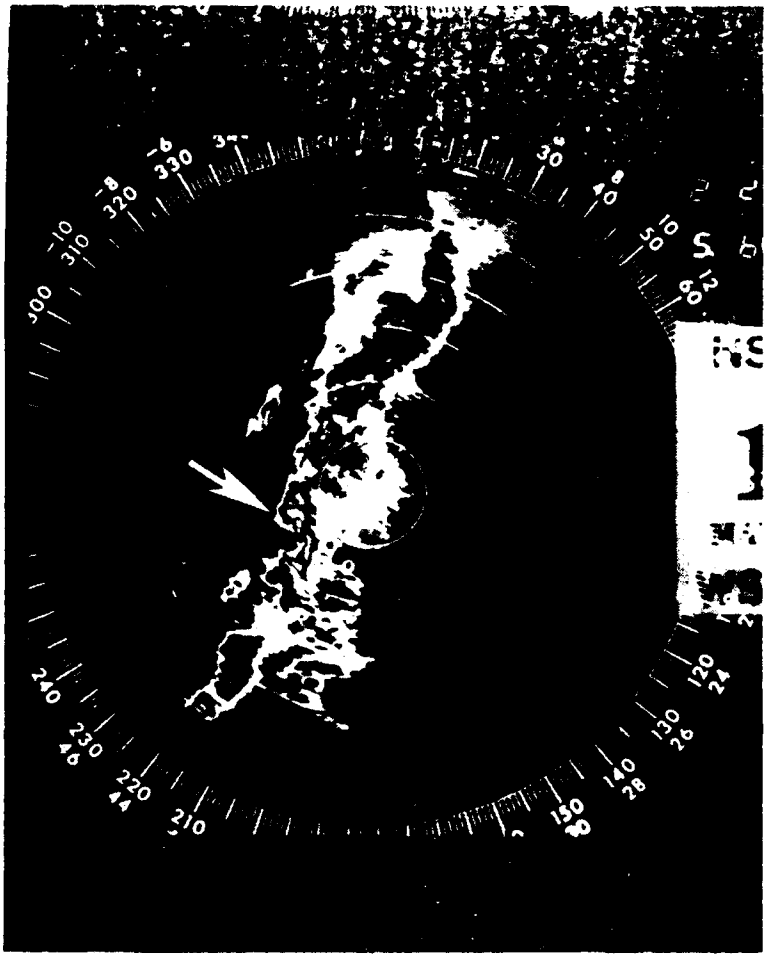

Figure 3 NSSL WSR-57 radar scope photgraph for 1628CST 17 May 1983. Elevation angle is 0.2 deg. Range marks are at 40km intervals. Echo contour levels are at 10dBZ intervals starting at 20dBZ. Storm studied is indicated by arrow.

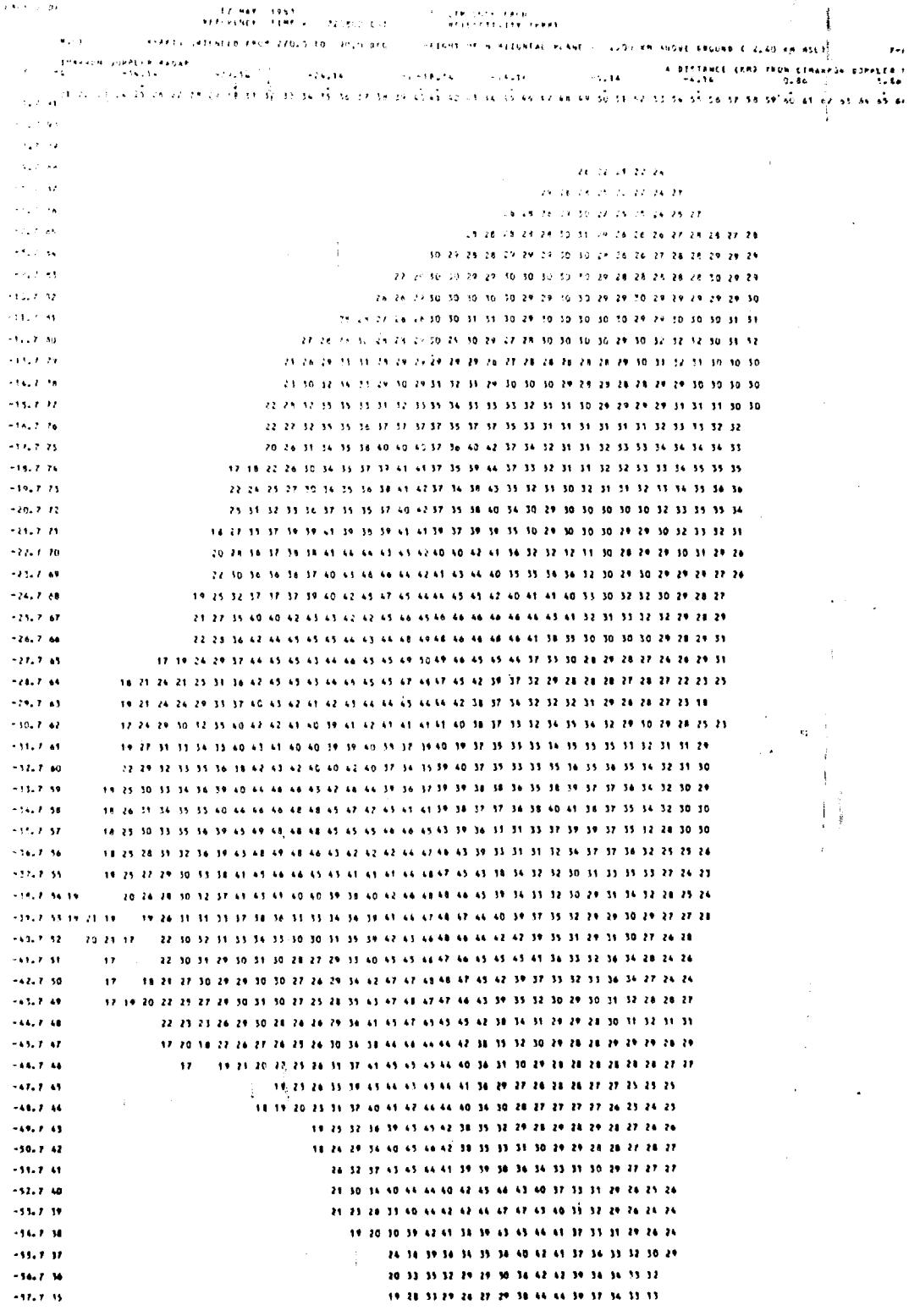

Figure 4 Section of the computed radar reflectivity (in dBZ) at 2km AGL. 17 May 1983 1628CST as seen by CIM. Spacing of data points is 1km.

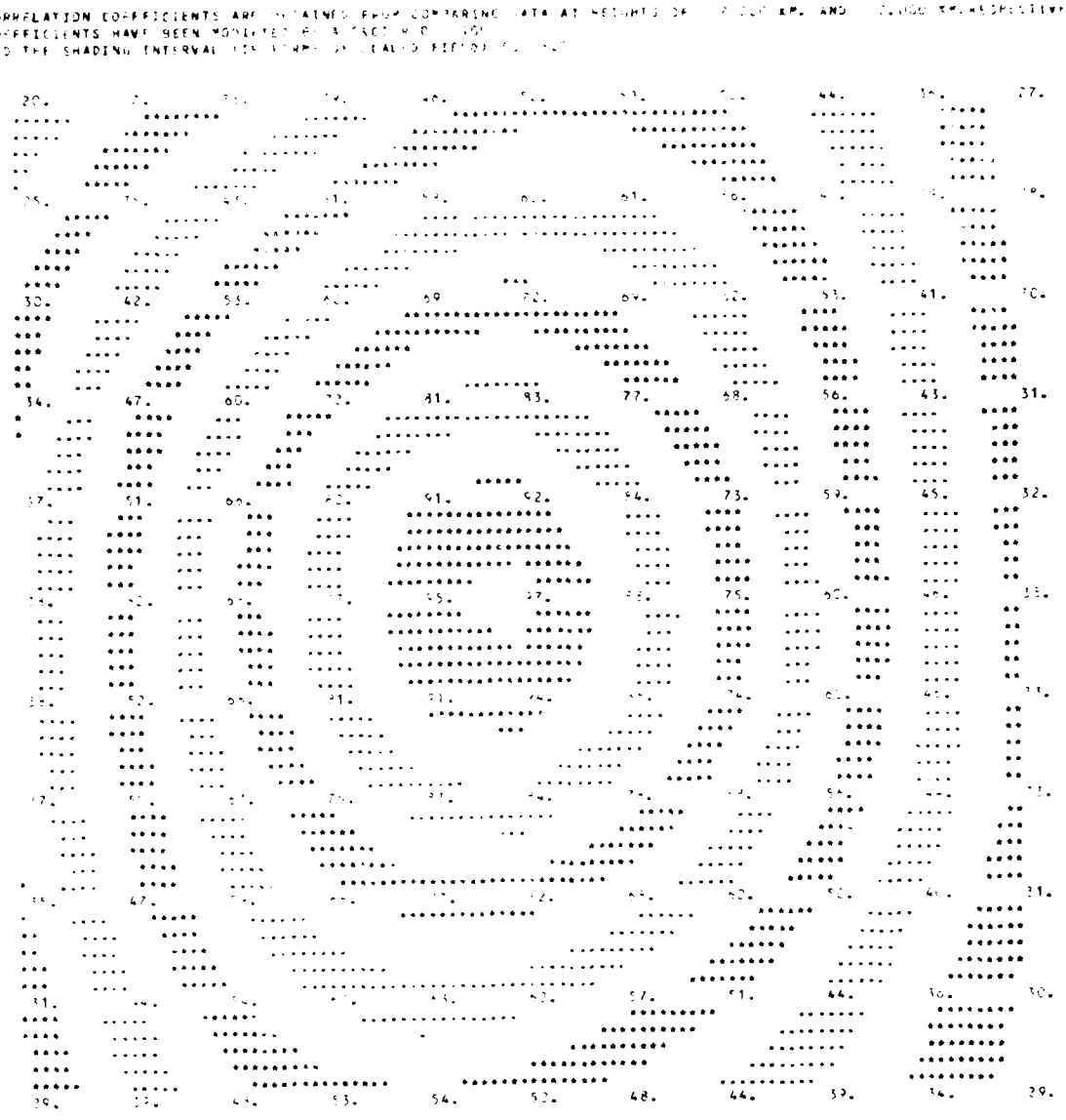

Figure 5 Correlation coefficients for CIM-NRO reflectivity field at 2km 17 May 1983.

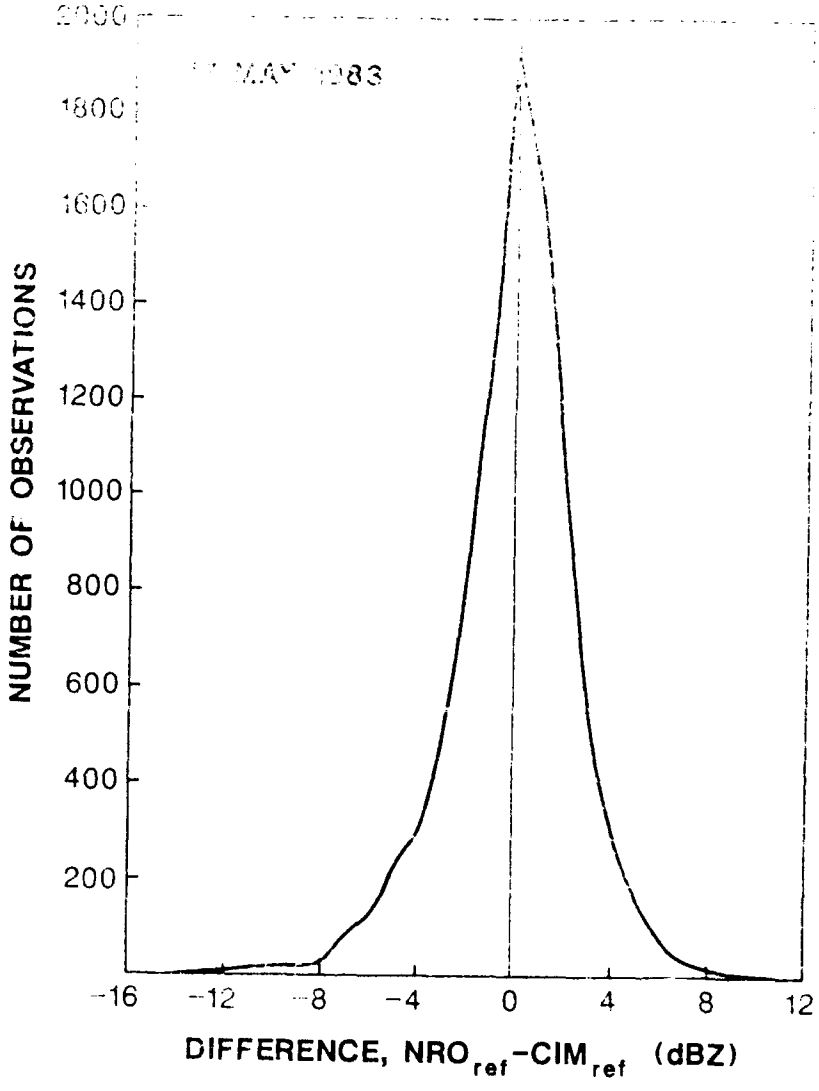

Figure 6 Distribution of reflectivity differences (dBZ) between NRO and CIM for all altitudes 17 May 1983 1628 CST.

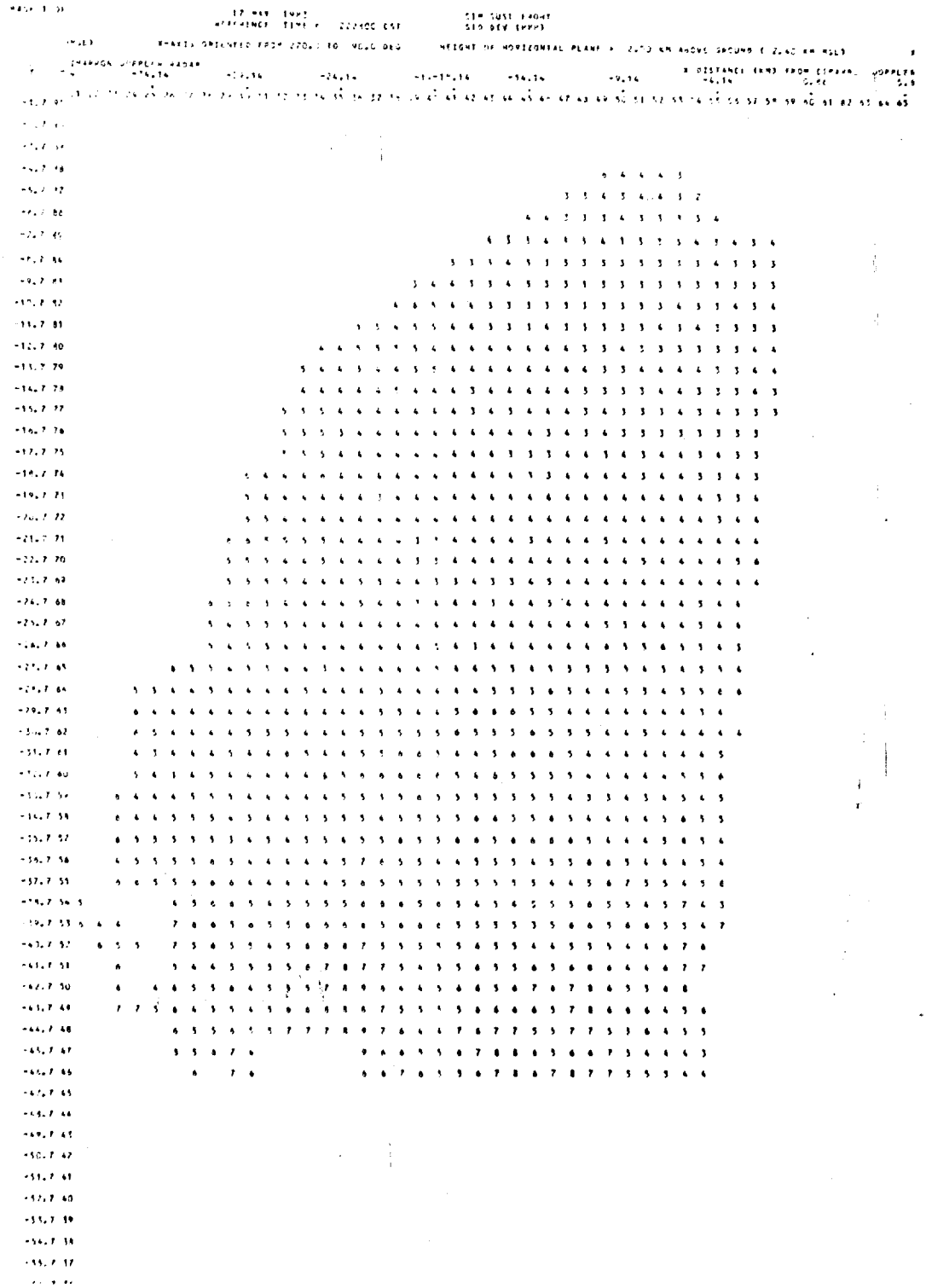

Figure 7 Section of computed CIM spectral widths (ms-1) at 2 km 17 May 1983 1628 CST. Data are at 1 km intervals.

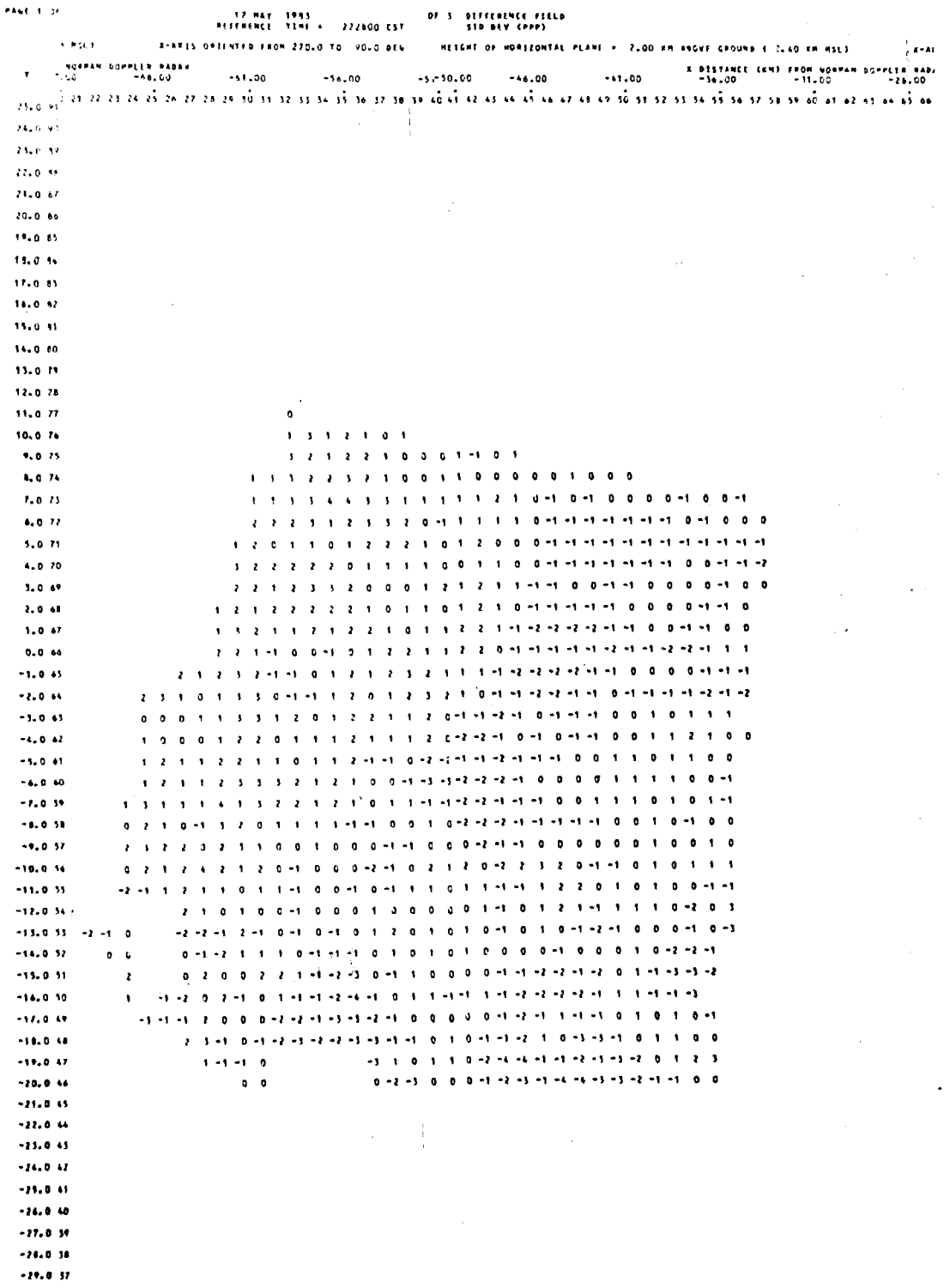

Figure 8 Spectral width differences (ms-1) at 2 km 17 May 1983 corresponding to area in Figures 4 and 7.

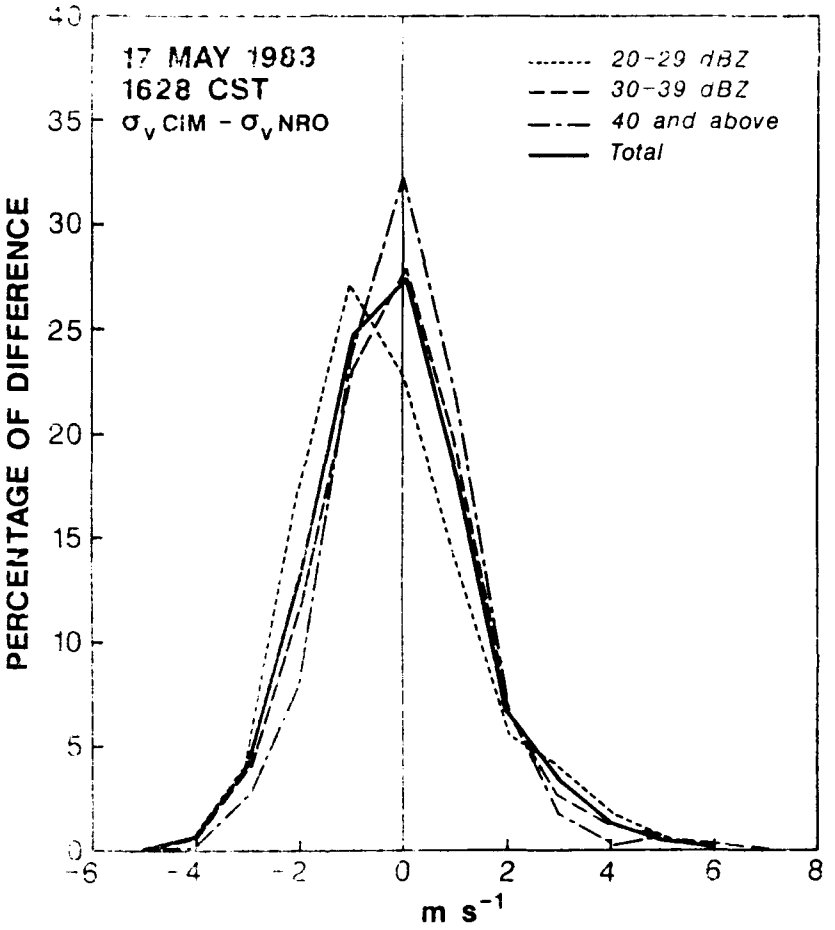

Figure 9 Summary of spectral width differences between NRO and CIM for all altitudes combined. Shown is the distribution of the 8500 data points quantized by reflectivity at 20-29dBZ, 30-39dBZ and over 40dBZ. In addition the combined distribution is shown with a heavy black line.

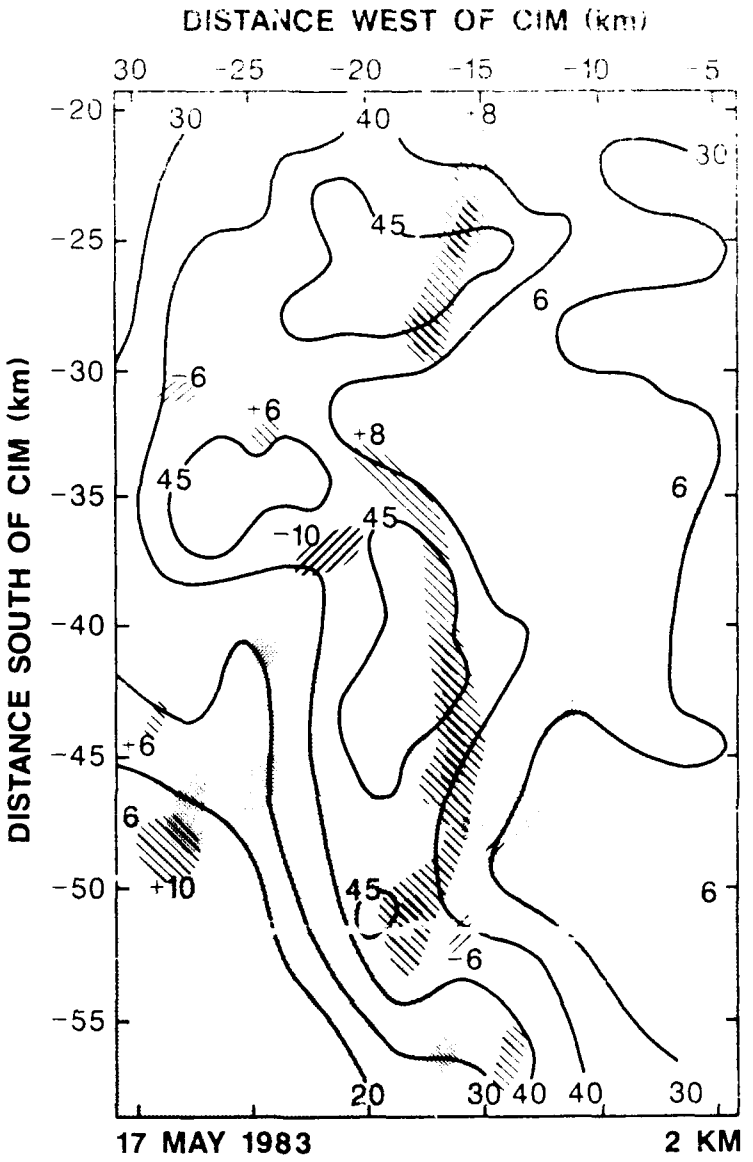

Figure 10 17 May 1983, 1628CST, 2km level with hatched areas showing vertical motion centers of 6ms-1 or more, and dotted areas corresponding to spectral widths regions of 6ms-1 or more. Solid contour lines indicate reflectivity levels (dBZ).

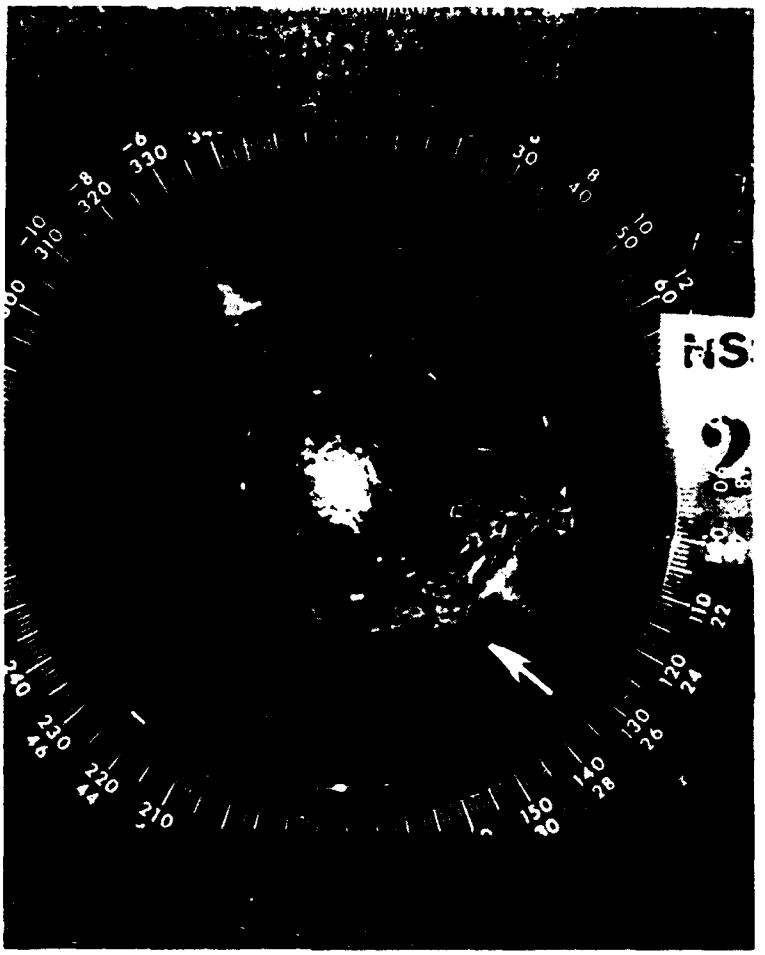

Figure 11 NSSL WSR-57 weather radar scope photograph 25 May 1983 1707 CST. Range marks at 40 km intervals. Reflectivity contours at 10dBZ intervals starting at 20dBZ. Arrow indicates storm. Numerous small echoes in photograph are from aircraft transponders showing location of aircraft.

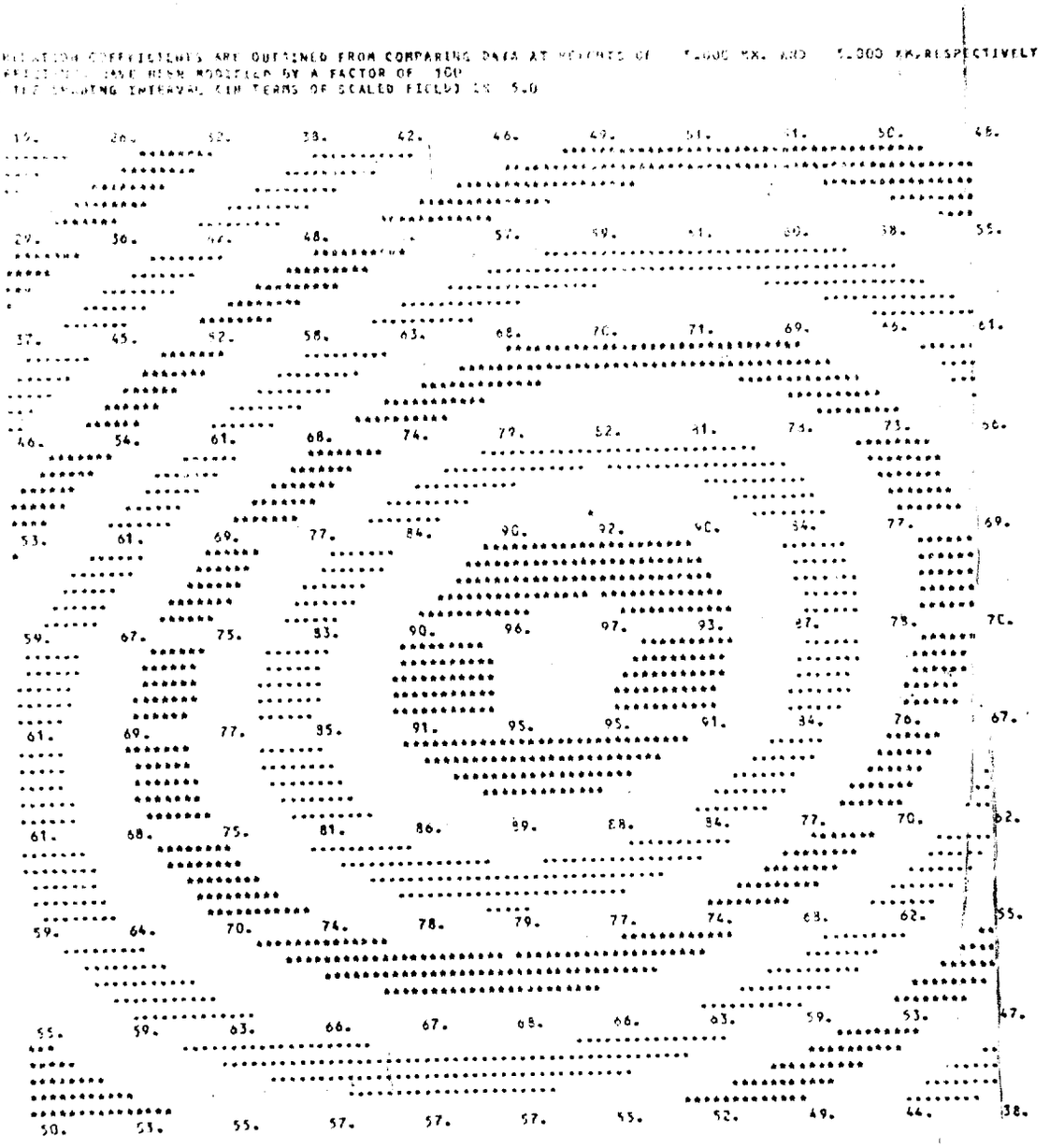

Figure 12 Cross correlation coefficients between NRO and CIM reflectivity fields for 5km 25 May 1983 1707 CST.

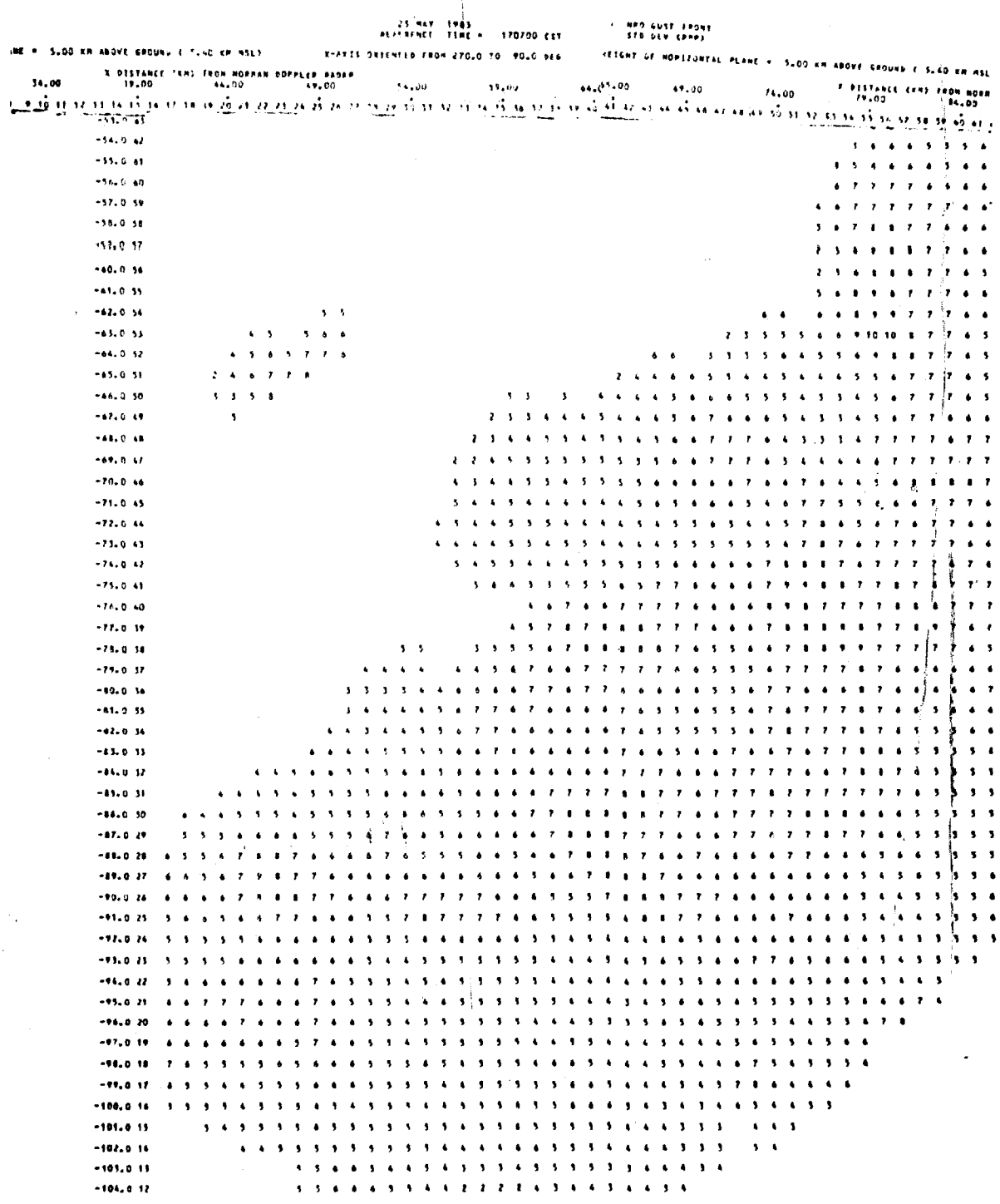

Figure 13 Section of computed NRO Doppler radar spectral widths (ms-1) for 5 km 25 May 1983 1707 CST. Data are at 1 km intervals.

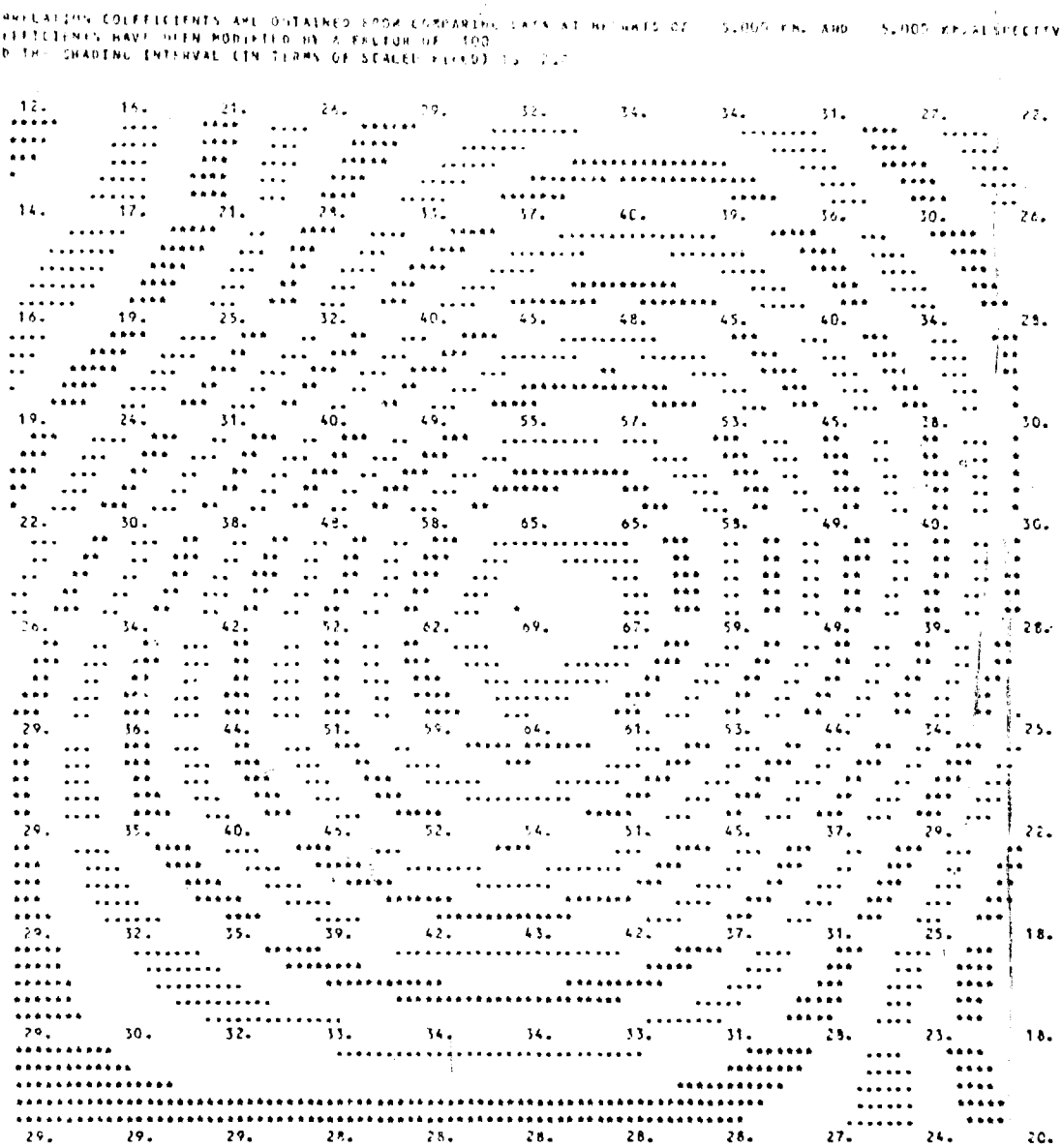

Figure 14 Cross correlation coefficients between NRO and CIM spectral width fields for the same scan as in Figure 12.

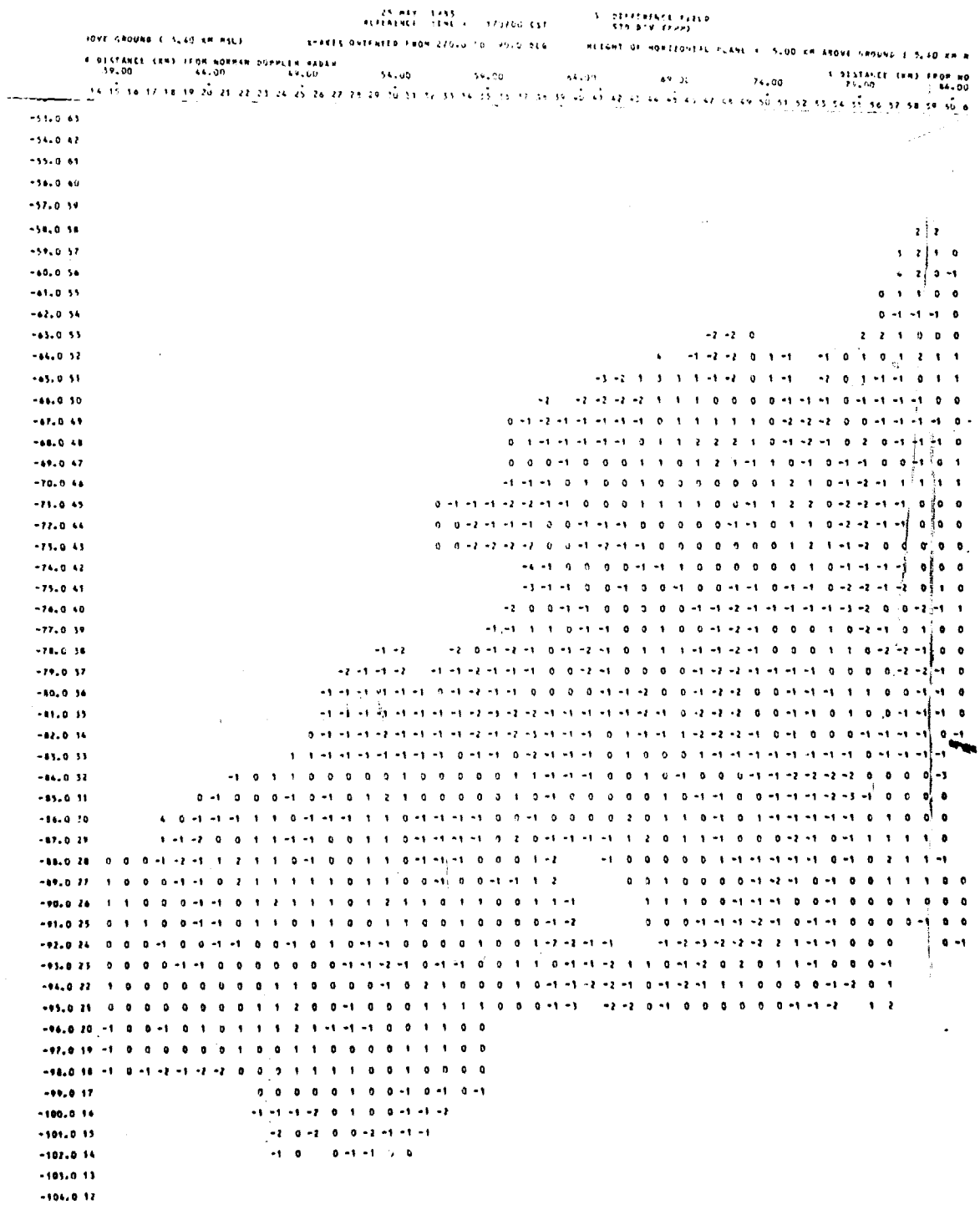

Figure 15 Section of spectral width differences (ms-1) between NRO and CIM at 5 km 25 May 1983 1707 CST.

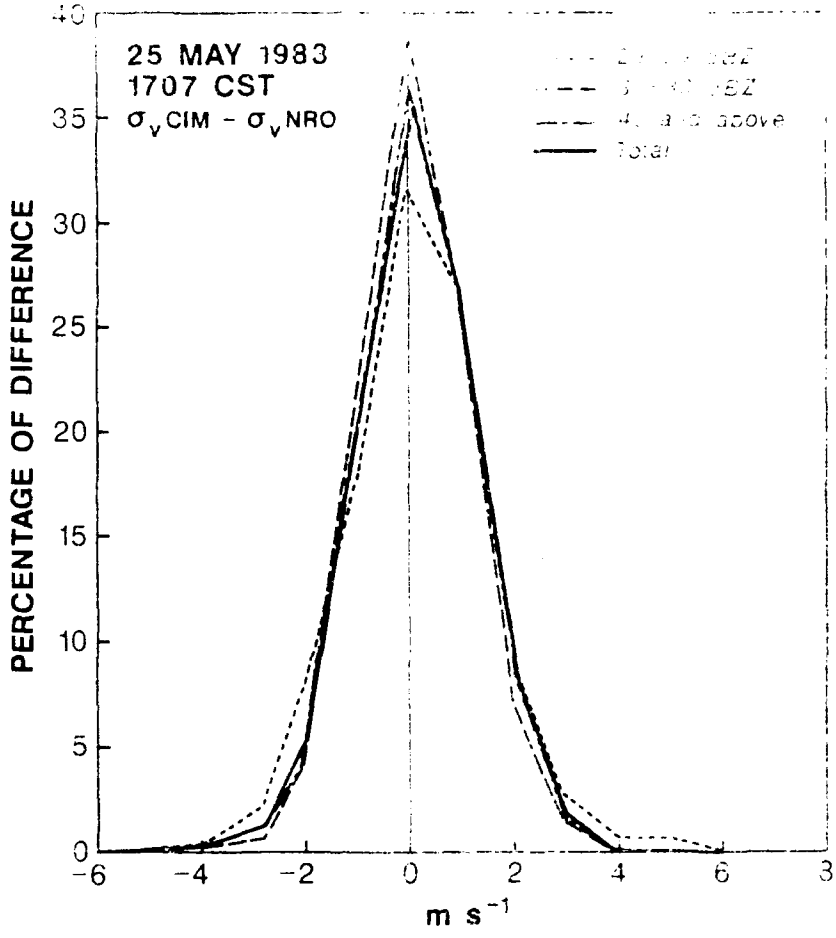

Figure 16 Summary of spectral width differences (ms-1) for all altitudes in storm 25 May 1983 1707 CST. Heavy dark line is the integrated value for all reflectiveness. (11,250 data points).

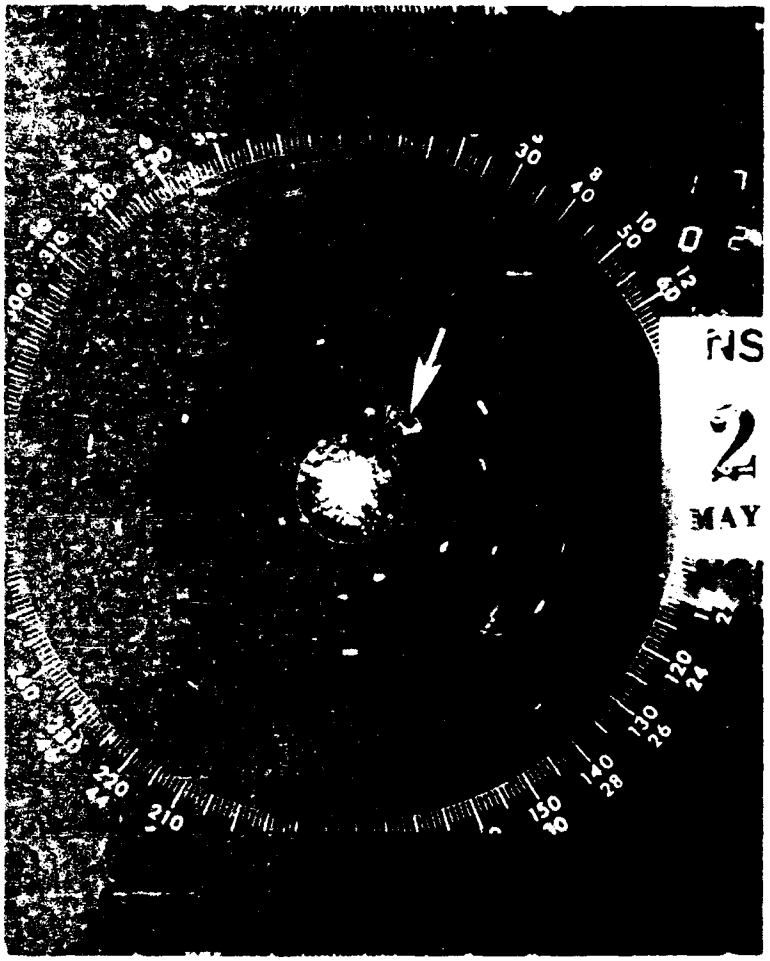

Figure 17 Similar to figure 11 except for 27 may 1983 1740 CST.

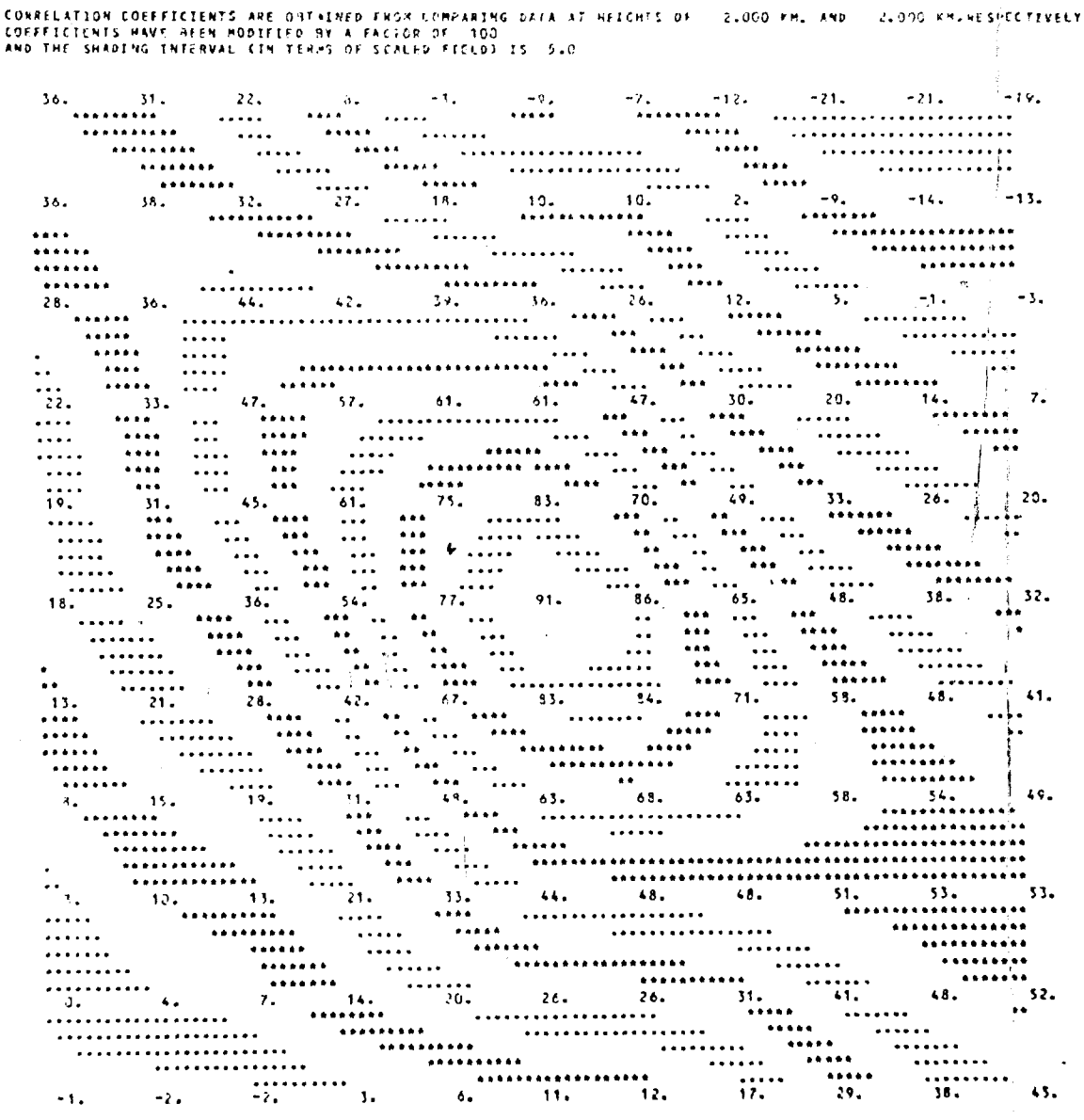

Figure 18 Cross correlation coefficients between NRO and CIM reflectivity fields for 2 km 27 May 1983.

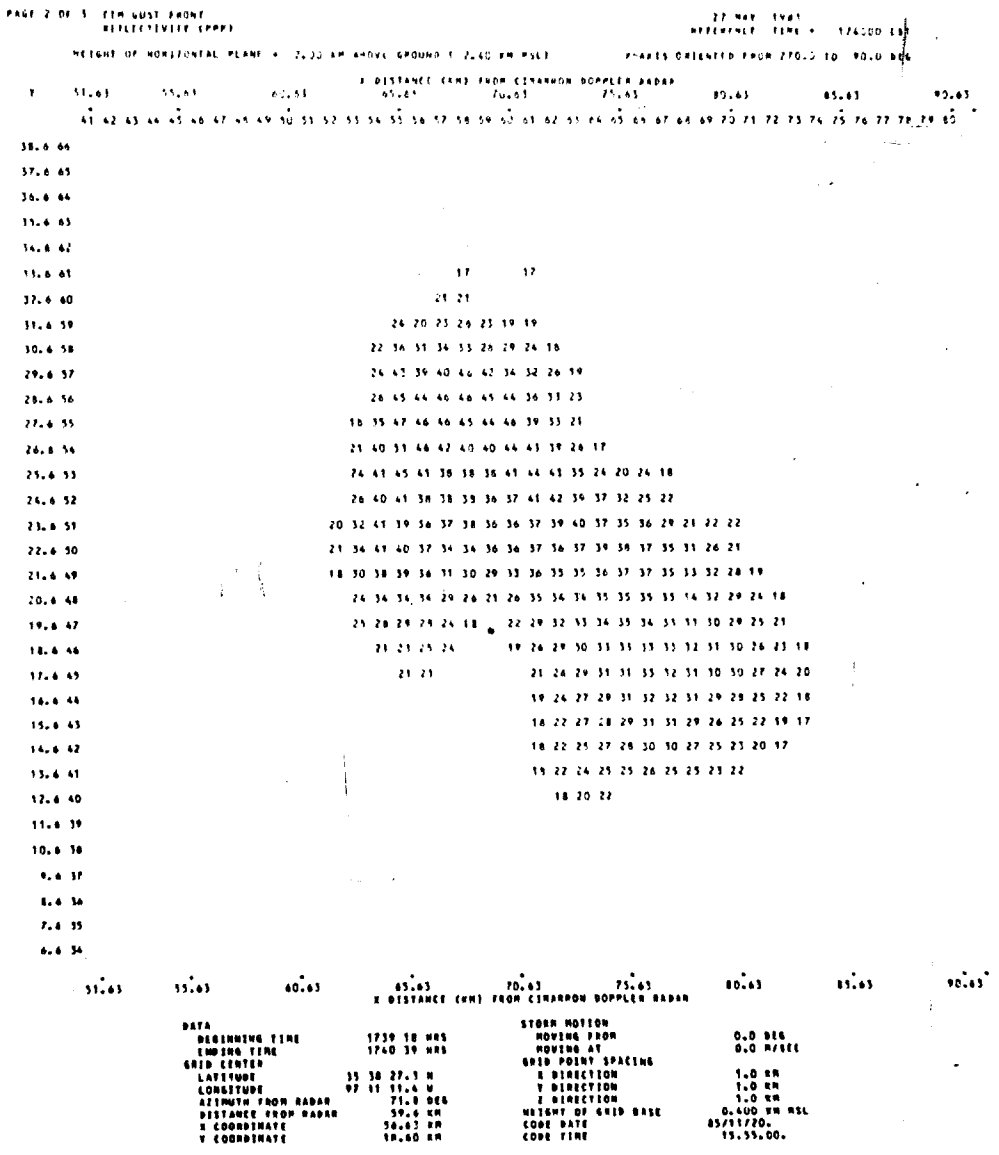

Figure 19 CIM reflectivities (dBZ) at 2 km 27 May 1983 1740 CST. Data are at 1 km spacing.

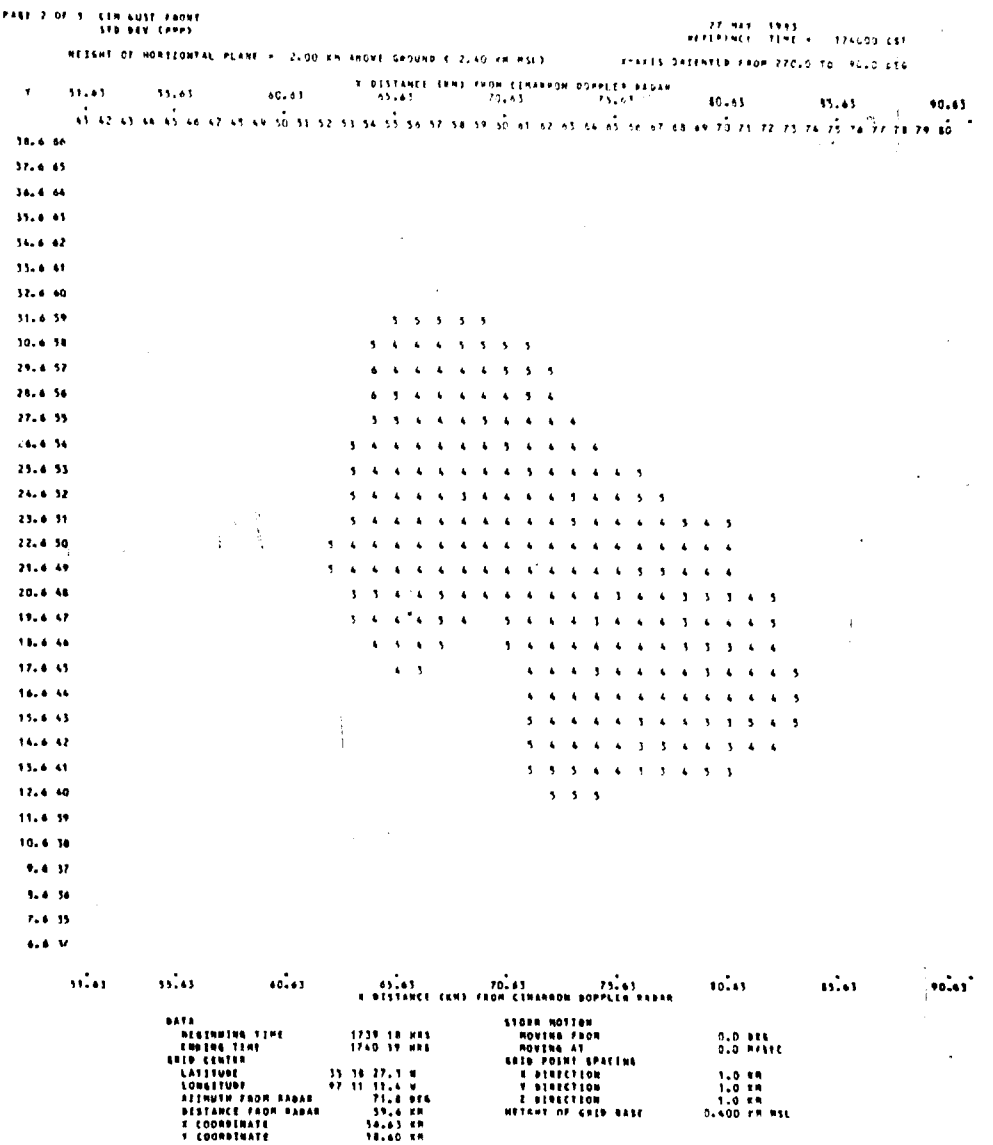

Figure 20 Computed 2 km spectral width field (ms-1) observed by CIM corresponding to figure 19.

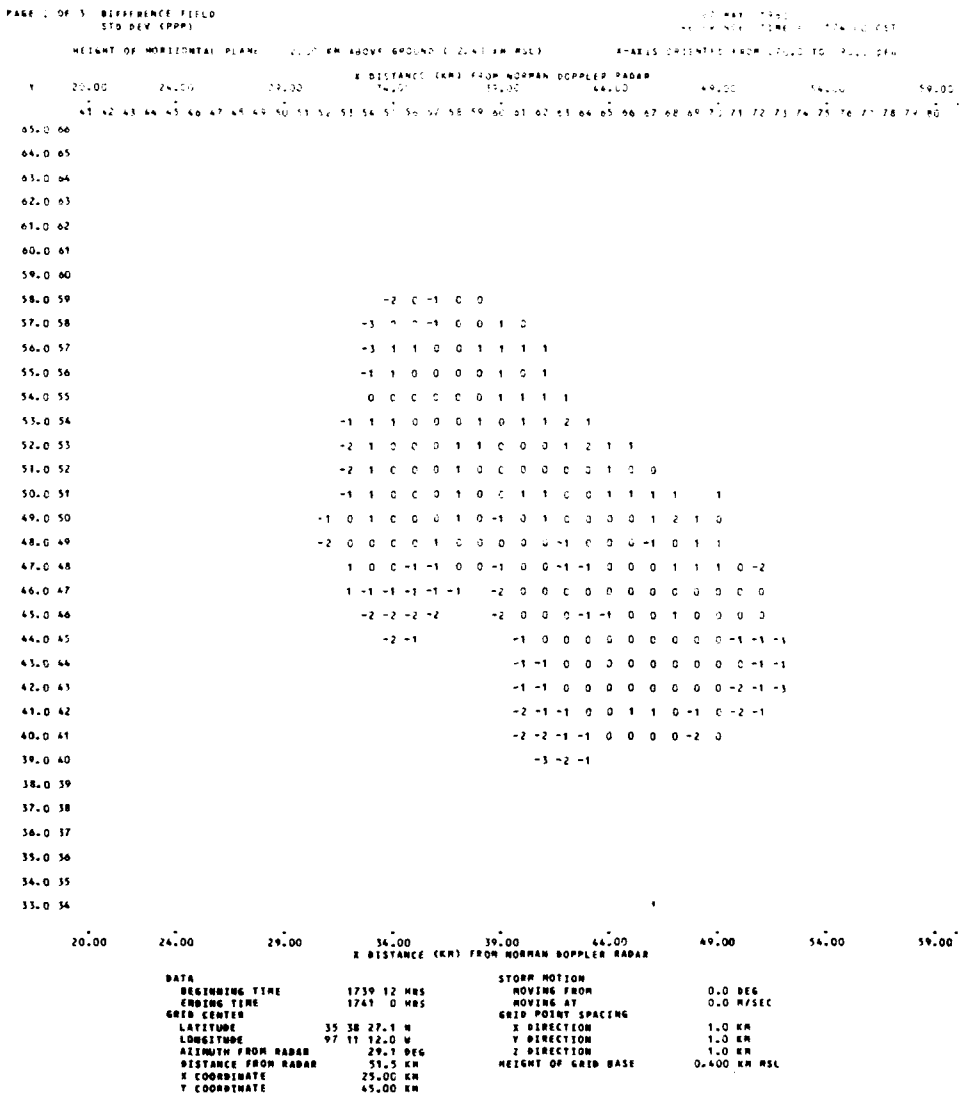

Figure 21 Spectral width differences (ms-1) between NRO and CIM at 2 km 27 May 1983 1740 CST.

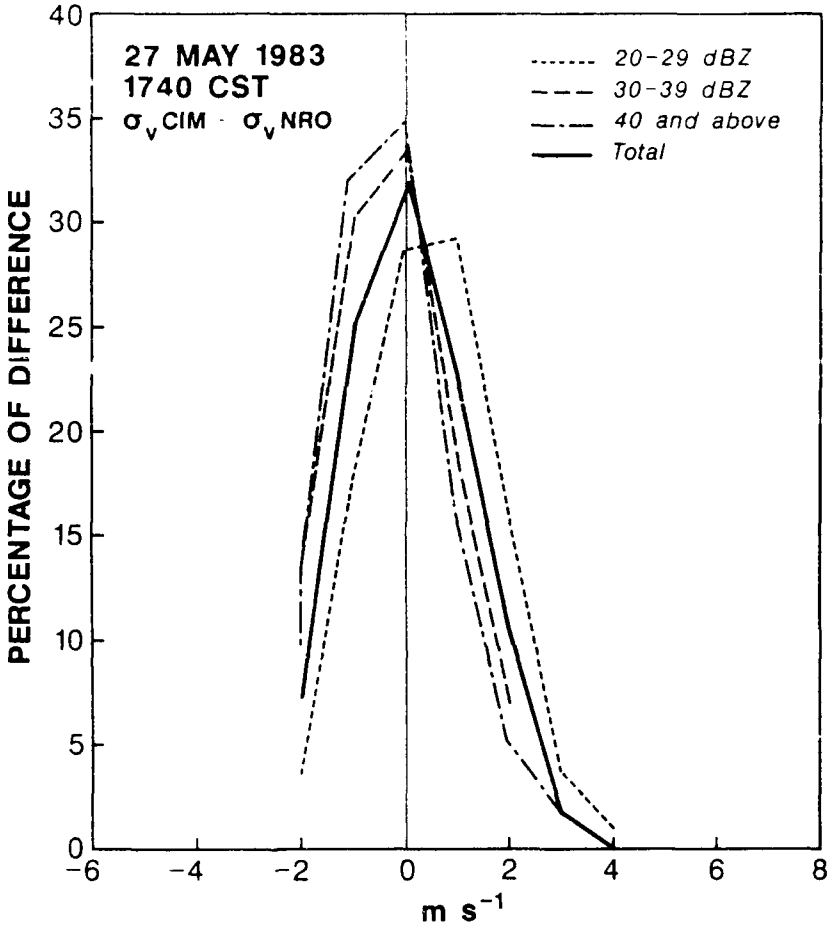

Figure 22 Summary of spectral width differences for all altitudes. Similar to figure 16 except for 27 May 1983. (720 data points).

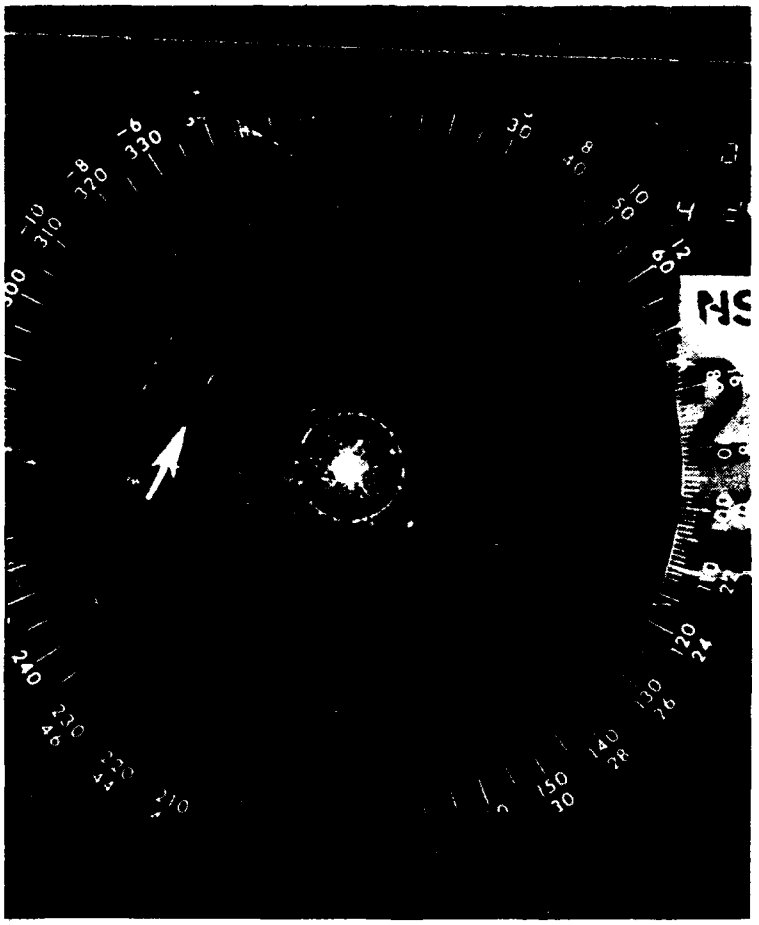

Figure 23 WSR-57 radar scope photograph similar to figure 11 except for 28 May 1983 2008 CST.

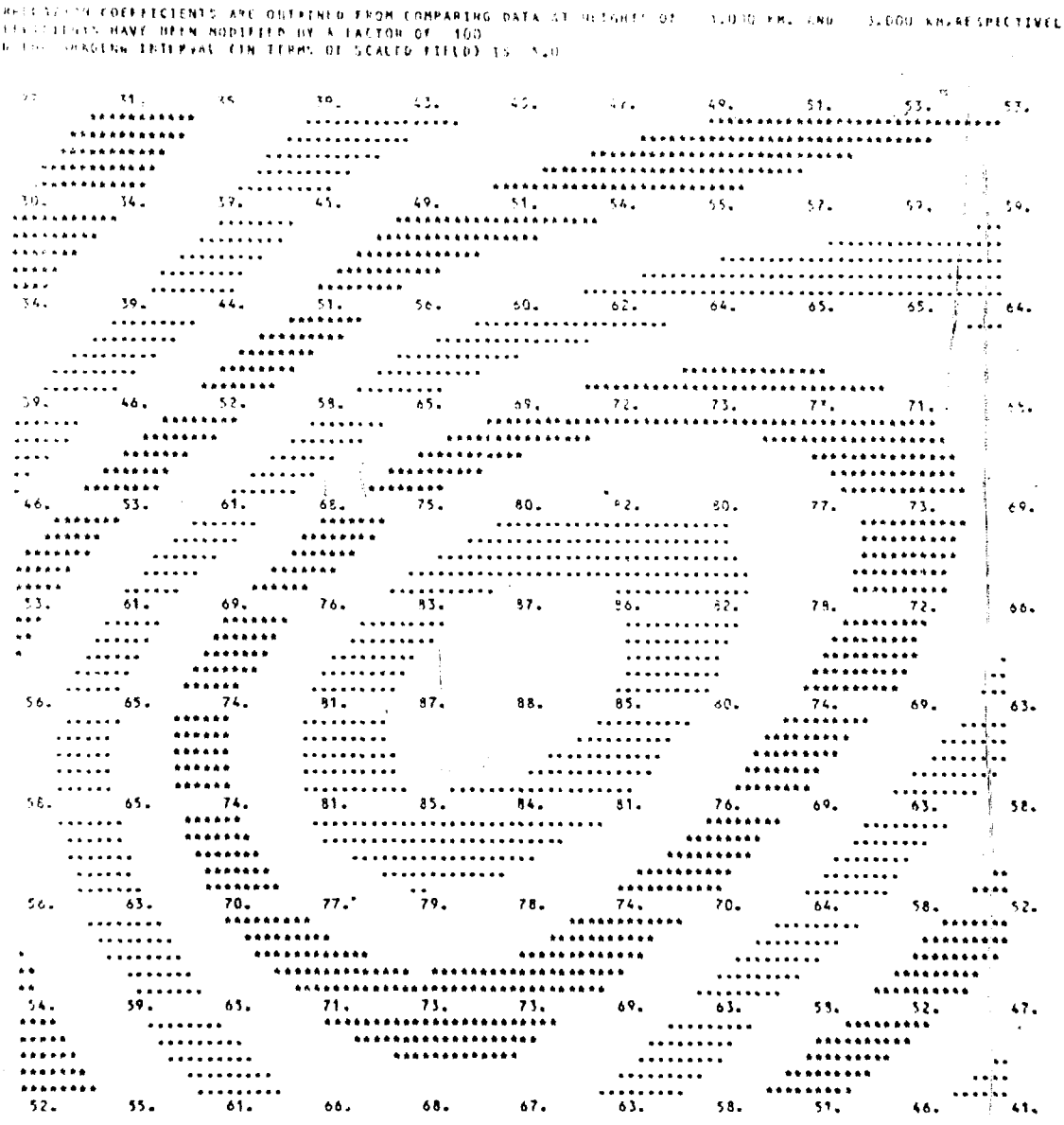

Figure 24 Cross correlation coefficients between NRO and CIM reflectivity fields at 3 km for 28 May 1983, 2008 CST.

Figure 25 Section of the CIM spectral width field at 3km 28 May 1983 2008 CST. Data are at 1 km intervals.

Figure 26 Spectral width differences (ms-1) between NRO and CIM corresponding to data in figure 25.

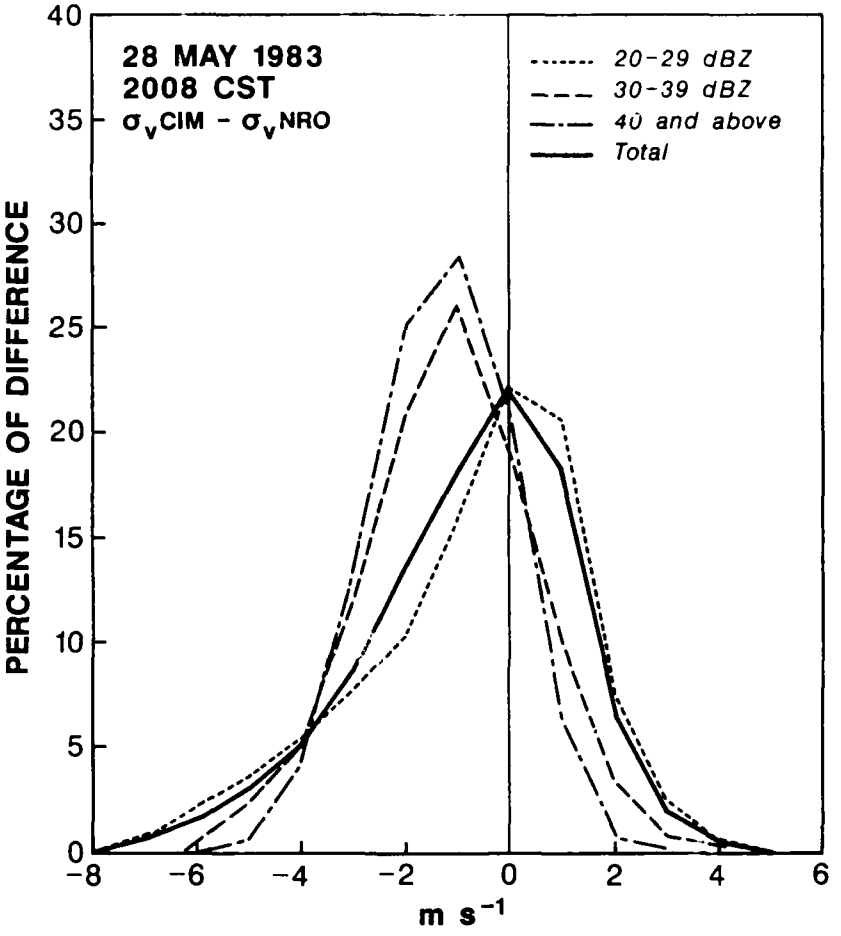

Figure 27 Summary of spectral width differences (ms-1) for all altitudes 28 May 1983 2008 CST occurring at specific dBZ intervals. Heavy dark line is the distribution for all reflectivities. (9,450 data points).

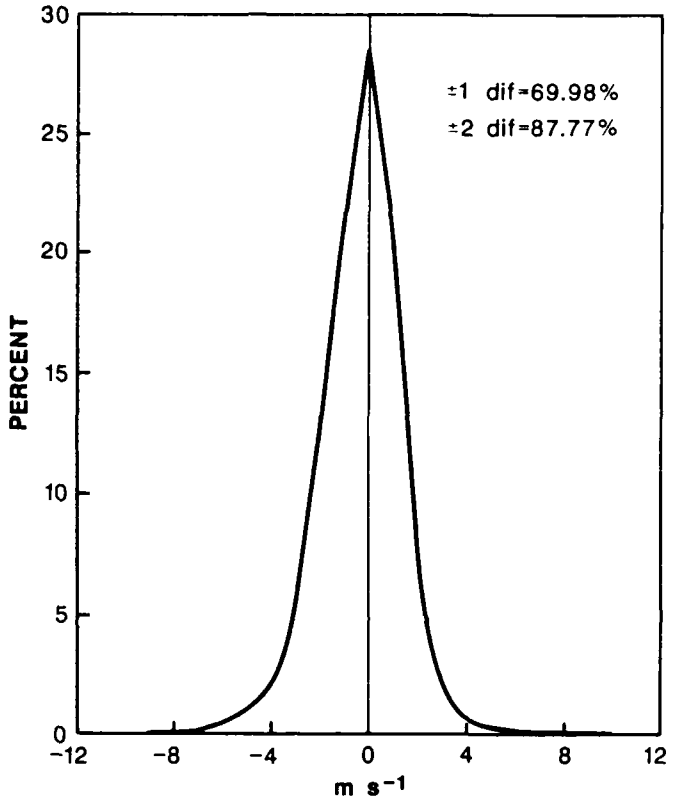

Figure 28 Composite of spectral width differences for the four storms. (29,850 data points).